Regulation of intracellular magnesium during human adenovirus infection

Alisha Gerrior

Department of Biochemistry

McGill University, Montreal

April 2021

A thesis submitted to McGill University in partial fulfillment of the requirements of the degree of Master of Science.

Table of contents

Table of Tables

Table of Figures

List of Abbreviations

Ad2	human adenovirus serotype 2
Ad5	human adenovirus serotype 5
Akt	protein kinase B
CAR	coxsackie B virus – adenovirus receptor
CBS	cystathionine-β-synthase
cGAS	cyclic GMP-AMP synthase
CNNM	cyclin M, ancient conserved domain protein
CPE	cytopathic effect
DAPI	4’,6-diamidino-2-phenylindole
DBP	HAd DNA binding protein
dFBS	dialyzed fetal bovine serum
DMEM	Dulbecco’s Modified Eagle Medium
E1A	Ad5 early protein A1
E4orf4	Ad5 early protein 4 open reading frame 4
E4orf6	Ad5 early protein 4 open reading frame 4
EGFP	enhanced green fluorescent protein
ERK	extracellular signal-regulated kinase
EtOH	ethanol
FBS	fetal bovine serum
FFU	focus forming assay
HA	hemagglutinin
HAd	human adenovirus
HeLa-fLUCcp	magnesium sensitive reporter cell line, HeLa cells stably expressing PRL2 5’ UTR with destabilized firefly luciferase
hpi	hours post infection

hpt	hours post transfection
IFN	human interferon
IFNAR	interferon alpha/beta receptor
ISG	interferon stimulated genes
IRF1	interferon regulatory factor 1
JAK	Janus kinase
MOI	multiplicity of infection – viruses per cell
MWCO	molecular weight cut-off
PBS	phosphate buffered saline
PIK3	phosphoinositide 3-kinase
PP2A	protein phosphatase 2A
pRB	retinoblastoma protein
PRL	phosphatase of regenerating liver protein
pSTAT1	phosphorylated signal transducer and activator of transcription 1
PTEN	phosphatase and tensin homolog
PTP	protein tyrosine phosphatase
PVDF	polyvinylidene fluoride
RuvBL1	RuvB-like AAA ATPase
STAT1	signal transducer and activator of transcription 1
STING	stimulator of interferon genes
TBST	tris(hydroxymethyl)aminomethane buffered saline with 0.5% Tween 20
TNF	tumor necrosis factor
TRPM7	transient receptor potential melastatin 7
uORF	upstream open reading frame
UTR	untranslated region

Abstract

Magnesium is required for many host cell processes, and thus may play an important role during infection, when the host cell is hijacked in order for the virus to replicate. Depletion of magnesium *in vitro* leads to a decrease in human adenovirus serotype 5 (Ad5) replication, however increasing extracellular magnesium levels does not confer an advantage. Ad5 early protein 4 open reading frame 4 (E4orf4) has been shown to target the CNNM3/PRL2 complex, which is potentially involved in intracellular magnesium homeostasis, and so to better understand the importance of this interaction, the role of E4orf4 during infection was characterized by looking at differences in relative genome copy, titer of replication and protein expression at physiological and lower than physiological magnesium conditions. Loss of E4orf4 leads to higher relative genome copy number, but this does not lead to higher replication efficiency. E4orf4 also assists with the early to late gene transition, so loss of E4orf4 leads to higher expression of early viral proteins, where magnesium seems to play more of a role. When using a magnesium sensitive reporter cell line, infection with either wildtype or E4orf4 null Ad5 causes alterations in the intracellular magnesium concentration, which is not seen with transfection of E4orf4 alone, or co-transfection with E4orf4 and CNNM3. To determine if the host cell immune response plays a role in this alteration, the reporter cell line was stimulated with interferon, but no significant alteration was found. While promising, further optimization of the magnesium sensitive reporter cell line is needed to determine which pool of intracellular magnesium is being sensed, along with validation to show that alterations in the intracellular magnesium levels are biologically relevant.

Résumé

Le magnésium est un élément requis dans plusieurs processus cellulaires. Ceci pourrait l'amener à être un joueur important lors d'une infection surtout lorsque la machinerie de la cellule hôte est détournée en faveur de la réplication d'un virus. En effet, l'élimination, *in vitro*, du magnésium résulte en la diminution de la réplication de l'adénovirus humain de sérotype 5 (Ad5) alors que l'augmentation des niveaux extracellulaires de magnésium n'apporte pas d'avantage. Il a été démontré que le gène précoce de la région E4 dans le cadre de lecture ouvert 4 de l'Ad5 (E4orf4) cible le complexe protéinique CNNM3/PRL2, complexe potentiellement impliqué dans l'homéostasie intracellulaire du magnésium. Afin de mieux comprendre l'importance de cette interaction, le rôle joué par E4orf4, durant l'infection, a été étudié, dans des conditions de concentrations physiologiques ou plus basses de magnésium, en déterminant les différences au niveau: du nombre de copies relatives du génome, de la titration de la réplication et de l'expression des protéines. Dans ces contextes, l'absence d'E4orf4 se traduit par un nombre plus élevé de copies relatives du génome mais pas par une augmentation de l'efficacité de la réplication. Le fait que E4orf4 facilite la transition de l'expression des gènes précoces vers les gènes tardifs, cause une augmentation de l'expression des protéines virales précoces lorsqu'il n'est pas exprimé; condition dans laquelle le magnésium semble jouer un rôle plus important. Lorsqu'une lignée cellulaire exprimant un rapporteur sensible au magnésium est utilisée pour une infection faite soit par l'adénovirus de type sauvage ou par celui n'exprimant pas E4orf4, on observe des changements au niveau de la concentration intracellulaire de magnésium. Par contre, si E4orf4 est transfecté dans ces mêmes cellules, seul ou en combinaison avec CNNM3, aucune modification n'est observée. Afin

de déterminer si la réponse immunitaire de la cellule hôte joue un rôle dans ces changements, la lignée cellulaire exprimant le rapporteur sensible au magnésium a été stimulée avec de l'interféron. Aucune modification significative n'a été trouvée. Bien que prometteuse, une optimisation plus poussée de la lignée cellulaire exprimant le rapporteur sensible au magnésium est requise afin que l'on puisse déterminer quel bassin intracellulaire de magnésium est détecté en plus d'une validation pour démontrer que les variations des niveaux intracellulaires de magnésium mesurées sont, biologiquement, pertinentes.

Acknowledgements

HeLa cells are derived from the cervical tumor of Henrietta Lacks without her knowledge or consent. My project involved the use of HeLa cells as a model cell line and I want to acknowledge Henrietta Lacks for her contribution.

I am thankful for the opportunity to study at McGill University, which is situated on the territory of the Kanien'kehà:ka. I would like to thank Dr. Jose Teodoro for accepting me into his lab. His passion for adenovirus was infectious, and I really enjoyed working on this project and getting to learn so many virology techniques. I would particularly like to thank the best research assistant in the world, Isabelle Gamache, as she was so supportive and helped me develop as a scientist. She answered my questions non-judgementally, and encouraged me when difficulties arose. Thank you to my Research Advisory Council members Dr. Selena Sagan and Dr. Michael Tremblay, who was our collaborator for this project.

It was honestly such a pleasure to work with the Teodoro and Tremblay labs. I would especially like to thank my amazing labmates Serena, Cynthia, Yilin, Owen, Mohamed, Michaela and Paola as you made coming to work such a joy and I would not have gotten through this degree without your love and support. Thank you for your willingness to listen and collaborate, I will miss working beside you. Thank you to my family Dolly, Patrick, Liam and Santokh and all my friends from home, even though I am horrible at explaining my work you always encouraged me. Finally, I would like to thank my partner Mohsin as you provided so much support, listened to every complaint about my misbehaving experiments and acted as the audience for every presentation I ever practiced.

1. Introduction

1.1 Human Adenovirus

Human adenovirus (HAd), of the family *Adenoviridae*, genus *Mastadenovirus*, was first isolated by Rowe and colleagues in 1953 from adenoid tissue [1]. HAd infection can lead to acute respiratory disease, conjunctivitis, and in some cases gastroenteritis, depending on the serotype. Infection spreads through close personal contact, which is why transmission is common through schools, daycares and in military bases. Due to its stability and infectivity, HAd has be used as a viral vector for gene transfer, and for vaccine development [2].

The discovery of HAd has since led to the classification of more than 70 serotypes. The types are based on antisera, and separated into subgroups based on hemagglutination and oncogenicity in rodents. Viral entry is also subgroup specific, the fiber knob of the adenovirus capsid subgroups B and F interact with different host cell receptors. All HAd are non-enveloped, and contain linear, double stranded DNA [3]. This project uses HAd serotype 5 (Ad5), of subgroup C as the viral model, as Ad5 is one of the more common types of infectious HAd and has been widely studied [2]. Ad5 uses the coxsackie B virus – adenovirus receptor (CAR) for cell entry. Once the virus undergoes endocytosis, the capsid begins to disassemble within the endosome, allowing viral DNA to enter the host cell nucleus and begin transcription [4].

1.2 Human Adenovirus Serotype 5 Genome

In order to maximise the amount of information carried by Ad5, the genome is polycistronic and contains multiple open reading frames, while the viral mRNA undergoes alternative splicing [5]. The expression of the Ad5 genome can be divided into early and late phases, with the division being viral DNA replication. Early genes (*E1-4*) are responsible for

preparing the host cell for infection, through the induction of DNA synthesis and downregulation of the host cell immune response [3,6]. The first viral gene expressed is *E1A*, which produces protein products that bind to pRB to release E2F, in order to move the host cell into S phase, allowing for viral DNA synthesis. E1A also helps to upregulate several viral early gene promoters [5,7]. Ad5 also produces proteins to help counteract cellular immune response pathways, such as the expression of host cell p53, through the expression of other early viral genes like *E1B* and *E3* [8]. Additionally, the viral genome is prepared for replication through the expression of viral *E2* gene products, like the DNA binding protein and adenovirus DNA polymerase [5,9].

Once viral DNA replication begins, viral gene expression transitions from early to late phase. This transition is facilitated in part by the *E4* gene products [10]. E4 open reading frame 4 (E4orf4) helps to downregulate the expression of early viral genes, and to facilitate alternative splicing of late mRNA. E4 open reading frames 3 and 6 (E4orf3, E4orf6) proteins assist in shuttling the viral mRNA to the cytoplasm for translation [5]. The 55K product of *E1B* (E1B55K) works with E4orf6 to degrade host cell proteins and shut down host cell protein production in favour of viral proteins [11–13]. Late viral genes are mainly responsible for capsid protein formation and assembly of the virion. In order to encourage the translation of viral over cellular mRNA, late viral mRNA contains a tripartite leader, which undergoes alternative splicing and lacks a secondary structure, allowing for ease of viral mRNA translation [14,15]. Once the capsid is assembled, the viral genome is packaged and the virus beings to accumulate in the nucleus. At this point, the cell starts to undergo cytopathic effect (CPE) due to the disruption of cellular

structural elements like intermediate filaments. This helps to permeabilize the host cell membrane, allowing for viral egress [16].

1.3 Development of Ad5 E4orf4 null, E1B55K null, and GFP-Ad5 Mutants

To study the effects of Ad5 proteins on the host cell, deletion mutants were created from the Ad5 wild type (WT) H5pg4100 first introduced by Groitl and Dobner (2007) [17]. Compared to the Ad5 reference genome described by Sugarman et al. (2003) [17,18], the H5pg4100 genome has a deletion from nucleotides 28593 to 30471 in the E3 region. Miron et al. (2009) [19] used the H5pg4100 backbone for the creation of E4orf4 null Ad5, leaving the other E4 gene products unaffected. Kindsmüller et al. (2009) [20] developed an E1B55K null Ad5 from H5pg4100 by introducing point mutations in E1B, creating premature stop codons in the region coding for the E1B-55K protein. The GFP-Ad5 mutant was created by Smadja-Lamère et al. (2008) [21] by subcloning FLAG-GFP into a HAd vector, as described.

1.4 Human Adenovirus Early Protein 4 Open Reading Frame 4

The viral protein E4orf4 is not essential for viral replication as E4orf4 null Ad5 (E4orf4-Ad5) are still able to replicate [21–23]. In the context of infection, E4orf4 assists with the transition from early to late viral gene expression. When comparing E4orf4- Ad5 infection to WT Ad5 there is an increase in expression of early genes, and a decrease in expression of late genes since the transition between early and late expression is disrupted [19,23,24]. When expressed alone, outside the context of a viral infection, E4orf4 is able to induce p53 and caspase independent apoptosis in p53-null cancer cells [22,25–27].

The interaction between host cell protein phosphatase 2A (PP2A) and E4orf4 is vital for E4orf4 functionality within the host cell [28,29]. E4orf4-PP2A dephosphorylates viral E1A to stop

the E1A dependent upregulation of early viral genes, as E1A activates viral promoters for *E2* and *E4*, thus reducing expression of early viral genes [10,23]. E4orf4-PP2A is also able to dephosphorylate transcription factor E4F, which regulates *E4* gene expression [6]. As well, E4orf4 assists with late viral gene expression via post-translational mechanisms. The E4orf4-PP2A complex can dephosphorylate the SR splicing factors in order to assist with alternative splicing of late viral mRNA, L1-IIIa, which also transitions viral gene expression to the late phase [23,30].

1.5 E4orf4 Interaction with Host Cell Proteins

The main interaction partner of E4orf4 is the host cell serine/threonine phosphatase PP2A. PP2A consists of a base dimer, made up of base subunit A and catalytic subunit C. To this base dimer binds subunit B, which gives PP2A substrate specificity and localization. There are 4 types of the B subunit, and each type is made up of several isoforms [22,31]. E4orf4 has been found to interact with mainly with subunit B55α [28,32]. In uninfected cells, PP2A assists in cell cycle progression, through dephosphorylating pocket proteins such as pRb and other kinases involved in mitotic exit [31,33,34]. Ad5 isn't the only virus to target PP2A, other viruses such as HIV-1, polyomavirus, Epstein-Bar virus and human papillomavirus also interact with PP2A in order to manipulate the host cell during infection [35]. To better understand the interaction and role of E4orf4-PP2A in the host cell, Marcellus et al. (2000) [30] created alanine substitution mutants of HA tagged HAd serotype 2 (Ad2) E4orf4. These mutants were divided into two classes; class I mutants are defective in their ability to bind PP2A and class II mutants are able to bind but are defective in their ability to induce apoptosis [30]. As HAd2 and HAd5 are under the same subgroup, and are highly similar in their E4 gene composition, these HAd2 E4orf 4 mutants can also be used to understand the role of HAd5 E4orf4 [36].

To further explore the interaction of E4orf4-PP2A with other host cell proteins, affinity purification mass spectrometry (AP-MS) was performed by Mui et al.(2015) [29]. In addition to PP2A, other interaction partners of E4or4 included family members of protein groups Cyclin M (CNNM1-4) and the protein tyrosine phosphatase family (PTA4A1-4), also referred to as phosphatase of regenerating liver (PRL1-3) [29]. For this project, the complex formed by isoforms CNNM3 and PRL2 are the focus, as these members are strong interaction partners, and are expressed in many human tissues [29,37].

1.6 Cyclin M Protein Family

The CNNM protein family (CNNM1-4), also referred to as the ancient conserved domain protein family, are plasma membrane proteins involved in intracellular magnesium homeostasis. The functionality of the CNNM family is yet to be elucidated; it is not clear if CNNM functions as a magnesium transporter or as a sensor for the levels of free intracellular magnesium [38–40]. CNNM family members are differentially expressed in human tissue, with CNNM3 mostly ubiquitous, with high expression in organs such as the heart, lungs, and spleen [41]. The CNNM family members CNNM2 and CNNM4 have also been linked to magnesium reabsorption in the kidneys and intestine, respectively [42,43]. Mutations in CNNM proteins are linked to diseases involving magnesium wasting. CNNM2 mutations have been linked to familiar primary hypomagnesemia, as well as leading to issues with brain development and neuro-psychiatric disorders. Deletion of CNNM2 in mouse models has been shown to be embryonically lethal [44,45]. CNNM4 mutations lead to Jalili syndrome, characterized by amylogenesis imperfecta and cone-rod dystrophy [46].

The overall structure of the CNNM family consists of four major domains. The extracellular N terminal domain contains a signal peptide, and a conserved asparagine residue, which allows for plasma membrane localization for CNNM when glycosylated [41]. The transmembrane domain is a domain of unknown function (DUF21), which is linked to the cytosolic cystathionine-β-synthase (CBS) pair domain [38]. The CBS pair, or Bateman module, is a highly conserved region of CNNM that consists of two CBS domains that interacts within the pair, and allows the formation of a CNNM homodimer at the plasma membrane. This pair is able to undergo conformational changes due to interactions with other nucleotides, magnesium and proteins such as the PRL family[47–49]. The C-terminal consists of a cyclic nucleotide – binding homology (CNBH) domain, which is also well conserved between the isoforms, and may also be involved in the homodimerization and localization of CNNM at the plasma membrane [50,51].

1.7 Phosphatase of Regenerating Liver Family

The PRL protein family (PRL1-3) are dual specificity phosphatases that play a role in cell proliferation and mitosis. The family members share more than 75% of their amino acid sequence, and homologs of PRLs are present in all eukaryotes [52]. At their C terminus, all PRL family members contain a prenylation motif (CAAX box), preceded by a polybasic region. This domain is important for PRL biological function and localization. Prenylation of the CAAX box allows for localization of PRL to the plasma membrane, and deletion localizes PRL to the nucleus [53,54]. PRL1/2 are ubiquitously expressed in human tissue, with PRL3 mainly being expressed in the prostate, heart and muscle [53,55]. PRL2 specifically is linked to PI3K-Akt and ERK1/2 signalling, and knocking out PRL2 can lead to elevated PTEN levels and disruption on Akt

dephosphorylation [55]. However, PRLs have weak phosphatase activity, and many of their substrates are as of yet unknown [56,57]. As PRLs play a role in cell proliferation, overexpression of PRLs in cancerous tissue has been implicated in disease progression, from proliferation and invasion, leading to metastasis in both solid and liquid tumors [52,58–60]. The overexpression of PRLs in cancer cells may help to confer a metabolic advantage, allowing the cancer cell to meet the high metabolic demand required for proliferation and metastasis [61].

The expression of PRL is linked to the concentration of free intracellular magnesium in the cell, and levels of PRLs may be affected by the host circadian rhythm [61,62]. In mice, low dietary magnesium leads to an increase in PRL2 expression, with serum magnesium levels increasing in PRL2 deficient mice [55]. In a different study by Uetani et al. (2017) [62], this systemic magnesium deficiency has also been shown to cause weight loss, changes to body temperature, and metabolism. Under magnesium depletion, PRL2 protein levels increase, however there is no increase in mRNA, suggesting PRL protein expression is regulated through a post-translational mechanism [61,63]. Within the 5' untranslated region (UTR) of PRL mRNA there is a conserved upstream open reading frame (uORF), critical for the regulation of the main coding sequence. During translation, the current hypothesis by Hardy et al. (2019)[61] is that ribosomes stall at the first of two uORF start codons, preventing translation. However, this ribosome stalling is released when Mg^{2+} is depleted, increasing the rate of PRL mRNA translation and therefore increasing the PRL protein level in the cell [61].

1.8 Cellular Magnesium Regulation

The interaction of PRL and CNNM is linked to an increase in the intracellular Mg^{2+} concentration. CNNM may be acting as a pseudosubstrate for PRL, mediated by an aspartic acid

(D426) within the CNNM CBS domain, as well as residues within the catalytic pocket of PRL [59]. Individual PRL bind to each CNNM in the dimer, changing the conformation of the CBS pair which may be responsible for this increase in Mg^{2+}. Under low magnesium conditions, there is a higher association of PRL with CNNM, even though the levels of CNNM remain unchanged [42,61].

The PRL/CNNM complex is not the only intracellular complex potentially involved in cellular magnesium homeostasis. Magnesium plays a very important role in cellular processes; it acts as a cofactor for multiple enzymatic reactions, is needed to activate ATP and is required for protein and DNA synthesis. Most magnesium present in the cell is bound, with unbound levels ranging from 1-5% of total intracellular levels [64]. Magnesium deficiency *in vitro* leads to a suppression in cell growth, potentially by affecting the G1 to S phase transition [65]. In humans, a systemic chronic deficiency in magnesium has been linked to increased inflammation and oxidative stress, as well as an increased risk for developing certain types of cancer, muscular, neurological and cardiovascular issues among others [66–68]. The intracellular concentration of free Mg^{2+} is regulated in the cell by suspected transporters such as MagT1, Mrs2p, SLC41, and the ubiquitously expressed Transient Receptor Potential Melastatin 7 (TRPM7) [41,69,70]. TRPM7 may be activated when intracellular levels of magnesium are low, and like PRL2 it contains an upstream region on its mRNA that helps to regulate translation relative to intracellular magnesium levels [71,72].

1.9 Role of Magnesium in Viral Infections

As magnesium is vital for cell functionality, the link between magnesium and viral replication has been explored in several virus types, including Newcastle Disease Virus, Enterovirus and Rhinovirus, finding that the addition of magnesium during infection potentially

leads to enhanced viral replication [73–76]. For HAd specifically, a plaque assay was performed to look at changes in viral replication when increasingly higher than physiological amounts of magnesium chloride ($MgCl_2$) were used in the overlay media. The finding was that the rate of HAd release was increased with the extracellular supplementation of $MgCl_2$, up to 25mM [73]. These papers suggest there is a link between magnesium and the viral replication process.

1.10 Human Adenovirus Serotype 5 Infection and Cellular Antiviral Response

The initial response by the host cell to in response to Ad5 entry is through sensing of the Ad5 genome. In the cytoplasm, the innate cyclic GMP-AMP synthase (cGAS) and stimulator of interferon genes (STING) pathway, which acts like a DNA sensor, is activated by viral DNA. The cGAS/STING pathway leads to the activation of type 1 interferon (IFN) expression, specifically IFNβ [77,78]. In the nucleus, the Ad5 genome is sensed by the DNA damage response (DDR) pathway, as Ad5 DNA is linear with open ends and has a terminal protein, which is recognized by the DDR as a double stranded DNA break [77].

Interferons (IFNs) are cytokines that play a role in both innate and adaptive immune response to infection. Type I interferon, which includes IFNα and IFNβ are produced in the infected cell, and bind their cell surface receptor interferon-α/β receptor (IFNAR1/2) in order to activate the JAK/STAT pathway. This activation leads to the expression of interferon stimulated genes (ISGs), which are responsible for the antiviral effect [79,80]. Interestingly, Wolf et al. (1997)[81] have shown that stimulating cells through the addition of IFNα lead to an increase in cellular magnesium efflux, compared to unstimulated cells. Type II interferon, which includes IFNγ, are produced by immune cells in response to infection, and follow a similar pathway as type I IFN in order to activate ISGs [77,82].

In order to mitigate the cellular antiviral response, some Ad5 proteins target and block the induction of ISGs. Ad5 protein E1A interferes with the IFN signalling pathway by blocking STAT1 interaction with downstream protein interferon regulatory factor 1 (IRF1) by binding directly to STAT1, as well as decreasing the availability of proteins such as p300 and RuvBL1 which are needed to activate ISGs [77,83–85]. E1B, assisted by E4orf6, helps to inhibit apoptosis induced by the cellular antiviral response by targeting p53 for degradation, as well as other cellular proteins in order to stop the DDR pathway. It also interferes with the production of ISGs [83,86]. The E3 region also plays a role in antiviral response mitigation. The E3 glycoprotein gp-19K helps to inhibit the transport of the major histamine complex (MHC) to the cell surface. E3 proteins 14.7K and 10.4/14.5K help to further inhibit apoptosis induced by the Tumor Necrosis Factor (TNF) pathway [87]. Other proteins such as E4orf3 and VA RNA transcripts also help to block the cellular antiviral response.

1.11 Research Objectives

Viruses require functional host cells for their replication process, and the importance of magnesium for DNA replication and protein synthesis means magnesium plays a role in viral replication. The viral protein E4orf4, in complex with host cell phosphatase PP2A targets a host cell complex PRL-CNNM known to be involved in cellular magnesium homeostasis. The objective of this project is to determine the importance magnesium plays in viral replication, and if the Ad5 E4orf4 protein is responsible for alterations in intracellular magnesium concentrations over the course of infection. Previous unpublished work from our lab has shown that total magnesium is increased in cells infected with wild type Ad5. Similarly, we have shown

that E4orf4 targets the CNNM/PRL complex by interacting with CNNM3, which potentially undergoes dephosphorylation by PP2A.

2. Materials and Methods

2.1 Cell Lines

H1299 (NCI-H1299, ATCC CRL-5803), HEK293 (ATCC CRL-1573), and HeLa (ATCC CCL-2) cell lines were cultured in Dulbecco's Modified Eagle Medium (DMEM; Wisent) supplemented with 10% fetal bovine serum (FBS; Sigma Aldrich) and 1% gentamycin sulphate (Wisent). Cells were incubated at 37^{o}C with 5% CO_2. For cell maintenance in lower than physiological magnesium conditions, DMEM without $MgSO_4$ (Wisent) was supplemented with 5% dialyzed FBS (dFBS; Gibco), 1% gentamycin sulphate and 0.0081mM $MgSO_4$ (Wisent).

2.2 Adenovirus

Wild type adenovirus (H5pg4100, WT Ad5), E4orf4 null adenovirus (E4orf4- Ad5) and GFP conjugated Ad5 (GFP-Ad5) were developed by the labs of Dr. Thomas Dobner, and Dr. Phillip Branton [19,24]. All viruses used for this project are a gift from the lab of Dr. Philip Branton.

The WT and E4orf4- Ad5 were amplified in H1299 cells, in DMEM +/+ (FBS/gentamycin sulphate) at 37^{o}C with 5% CO_2. The cells were harvested, lysed, and purified using step then linear cesium chloride gradients (CsCl; Life Technologies) for density-based separation via ultracentrifugation (Optima L-80 XP Ultracentrifuge; Beckman Coulter). The CsCl was then removed by buffer exchange using 12-14 kDa MWCO dialysis tubing (Spectrum Laboratories Inc.) and titered using a focus forming assay.

For the kinetic luciferase assay infections, cell extracts of WT Ad5, E4orf4- Ad5 and E1B 55K null (E1B 55K-) Ad5 were used (a gift from Dr. Paola Blanchette).

2.3 Focus Forming Assay

H1299 cells seeded in a 12-well plate were infected with serial dilutions of virus in infection media (2% FBS, 0.2 mM $MgCl_2$, 0.2 mM $CaCl_2$ in 1X PBS) for 20 hours. The plates were washed once with PBS (1X) and fixed using ice cold methanol at -20^{o}C for 20 minutes. The plates were then washed once with 1X PBS, blocked and permeabilized in blocking buffer (10% FBS, 0.05% Triton X-100 in 1X PBS) for 1.5 hours at room temperature. They were incubated in 1:30 DNA Binding Protein (DBP, mouse monoclonal B6-8; Gift from Dr. Philip Branton) in blocking buffer, shaking for 1 hour, washed three times in PBS then incubated in 1:1000 Alexa Fluor-488 goat anti-mouse (Invitrogen) in blocking buffer, shaking for 1 hour [88]. The cells were stained with 4',6-diamidino-2-phenylindole (DAPI; Roche Diagnostics) for 5 minutes during the final PBS washes [89].

The plates were imaged using fluorescence microscopy (Axiovert 200M; Zeiss), with 5 images being taken per well, and performed in triplicate. The cells that fluoresce under FITC are manually counted using FIJI (ImageJ), and the average calculated for a final titer, based on the dilution, plate size and magnification strength (10X) [90,91].

2.4 Live Cell Imaging for Growth Curves

Triplicate 6-well plates were seeded with H1299 cells to a confluency of <10%. After 24 hours to allow for cell adherence, the media was changed to DMEM without $MgSO_4$, containing 5% dFBS and gentamycin, and supplemented with a dilution series of either $MgSO_4$ or $MgCl_2$

(Wisent). Live cell imaging was performed every 4 hours using the Incucyte S3 (Sartorius), at 37C and 5% CO_2, for up to a week.

2.5 Replication Assay

H1299 cells, either maintained at normal or low magnesium conditions (0.0081mM $MgSO_4$) where applicable, were seeded in 6-well plates for a confluency of 70-80% after 24 hours. The plating media was removed, and a low volume infection at MOI 5 was performed using DMEM -/- for 1 hour. This virus containing media was removed, and replaced with media containing varying amounts of magnesium, incubated for 28 hours post infection (hpi) or until cytopathic effect (CPE) was noted. The cells and supernatant were then harvested together and repeatedly frozen in a dry ice/ethanol bath then thawed in a 37^{o}C water bath to lyse the cells, releasing the virus into the supernatant. The supernatant was spun down to clear the cellular debris, and the titer of the resulting virus determined using the fluorescence forming assay.

2.6 Plaque Assay

GFP-Ad5 is lacking portions of the E1 and E3 regions, and are replication deficient unless infection occurs in HEK293 cells, which have been transformed using Ad5 specifically portions of the E1 region [92]. HEK293 were seeded to form a monolayer in 12-well plates 24 hours prior to infection. Low volume infection with a limiting number of virus particles was performed for 1 hour, with plate rotation to prevent drying every 15 minutes. The virus containing media was removed, plates washed once with 1X PBS and overlayed using 0.75% agar (Seaplaque; Lonza) containing 2.5X DMEM without $MgSO_4$ supplemented with 5% dFBS, 1% gentamycin, fungizone (Hyclone), and varying amounts of either MgSO4 or $MgCl_2$. Plaques were allowed to form for 7

days, after which fluorescence microscopy (Zeiss) was used to take stitched whole well images (MosaiX plugin; AxioVision) and the plaques counted and sized using the AxioVision Program (Zeiss).

For WT Ad5, HeLa cells were plated to create a monolayer in 6-well plates, 24 hours prior to infection. A low volume infection using limiting WT Ad5 particles was performed for 1 hour, with plate rotation every 15 minutes. The plates were then washed with 1X PBS, and overlayed using 0.75% agar containing 2.5X Minimal Essential Media (Gibco), supplemented with amino acids (50X MEM Amino Acid Solution; Wisent), vitamins (100X MEM Vitamins; Wisent), gentamycin, fungizone and FBS, as well as varying amounts of $MgCl_2$ [73,93]. The plaques were allowed to form for 7-10 days, after which the number of plaques per well were counted.

2.7 Immunoblotting

For protein expression experiments, H1299 cells were plated 24 hours prior to infection. To infect, the media was removed and replaced with E4orf4- Ad5 or WT Ad5 at MOI 5 in DMEM or with magnesium free DMEM for less than physiological magnesium infections. One hour post infection, the media was removed and replaced with DMEM supplemented with 10% FBS and 1% gentamycin for physiological or with magnesium free DMEM supplemented with 5% dFBS and 1% gentamycin for the less than physiological magnesium infections.

For immunoblotting, cells and supernatant were harvested at the required time point, pelleted and washed once with 1X PBS, then lysed using 1X Laemmli buffer. Samples were sheared using a 23G needle or by sonication (Bath Sonicator UCD-200; Diagenode Bioruptor) for 15 minutes, using a 30 second on/off cycle, then boiled for 5 minutes using a dry bath incubator (Fisher Scientific) set to 100^{o}C. Protein quantification was performed using the Pierce 660

Protein Assay and Ionic Detergent Compatibility Power for Pierce (ThermoFisher) and quantified by spectroscopy at 660nm (VarioSkan). Proteins were separated via gel electrophoresis using the TGX FastCast Gel Acrylamide Kit (Bio-Rad). All proteins except E4orf4 were transferred onto Low Fluorescence (LF) PVDF membranes (Bio-Rad) using the Trans-Blot Turbo Transfer System (Bio-Rad), then blocked with 5% milk in TBST. E4orf4 was transferred using the same system onto nitrocellulose membranes (Bio-Rad), then blocked with 5% BSA (BioShop) in TBST. Antibody blotting was performed using antibodies specific to the protein of interest, as listed in Table 1. Primary antibodies were diluted in 5% BSA in 1X PBS and secondary antibodies diluted in 5% milk in 1X PBS. Blots were visualized using Clarity Western ECL Substrate (Bio-Rad), and ClarityMax Western ECL Substrate (Bio-Rad) if required, and captured on the ChemiDoc XRS+ System (Bio-Rad). Western blots were analysed using the ImageLab 6.0.1 Software (Bio-Rad) to determine band and total lane protein intensity if applicable [94].

Table 1. Antibodies used for immunoblotting

Protein of Interest	**Primary Antibody**	**Supplier**	**Secondary Antibody**	**Supplier**
Ad Capsid	Rabbit Polyclonal L133[20]	Gift from Dr. Philip Branton	Goat anti-rabbit HRP	Jackson
CNNM3	Anti-CNNM3 Rabbit Polyclonal	Proteintech	Goat anti-rabbit HRP	Jackson
E1A	M73 Monoclonal Antibody [95]	Gift from Dr. Philip Branton	Goat anti-mouse HRP	Jackson
E4orf4	Rabbit Polyclonal 2419 [96]	Gift from Dr. Philip Branton	Goat anti-rabbit HRP	Jackson
E4orf6	Anti-E4orf6 Rabbit Polyclonal 1807 [97]	Gift from Dr. Philip Branton	Goat anti-rabbit HRP	Jackson
HA	Anti-HA Rabbit Polyclonal	Novus	Goat anti-mouse HRP	Jackson
FLAG	Anti-FLAG Monoclonal M2	Millipore Sigma	Goat anti-mouse HRP	Jackson
STAT1	Anti-Stat1 #9172	Cell Signalling	Goat anti-rabbit HRP	Jackson
pSTAT1 (Y701)	Anti-Phospho-Stat1 (Tyr701) # 9167	Cell Signalling	Goat anti-rabbit HRP	Jackson

2.8 Total Cellular Magnesium Quantification

H1299 cells were transfected using a 1:2.5 DNA to Lipofectamine 2000 (Invitrogen) ratio in Opti-MEM (Gibco) with HA-pcDNA3 as the empty vector, or with HA-E4orf4 wild type and HA-E4orf4 point mutants [30]. After 4 hours, the transfection media was replaced with DMEM +/+. The cells were harvested 48 hours post transfection, by centrifuging the supernatant and combining these cells with the scrapped cell pellet. The combined pellet was washed once with 1X TBS, suspended in 200µL TBS and split into 2 aliquots for ICP and WB analysis.

For analysis, the TBS suspended cells were placed into 15mL polypropylene tubes (SCP Science). The sample was digested using 0.5mL trace element grade HNO_3 (ThermoFisher) in a 100^{o}C bath for one hour, after which 0.5mL 30% H_2O_2 (BioShop) was added and the samples further boiled for one hour. Once cool, ddH_2O (MilliQ; Millipore Sigma) was used to adjust all samples to a final volume of 10mL. The digested samples were analyzed using Inductively Coupled Plasma – Optical Emission Spectrometry (ICP-OES iCAP 6000; ThermoFisher), calibrated to RQC1, phosphorus, sulphur, sodium and potassium standards (SCP Science). Samples were adjusted using a 1X TBS blank and normalized using the sulphur concentrations of the respective cell pellet sample, as sulphur levels are correlated to the protein concentrations in the sample [98].

2.9 Kinetic Luciferase Assay Using Magnesium Sensitive Reporter Cell Line

The intracellular Mg reporter cell line (HeLa-fLUCcp) used for this assay was obtained from Dr. Michel Tremblay. In brief, these cells stably express destabilized firefly luciferase downstream of the PRL2 UTR, linking firefly luciferase expression to changes in PRL2 UTR translation in response to varying intracellular magnesium [61,99].

For all assays, HeLa-fLUCcp were plated in a black, clear bottom 96-well plate (Costar) 24 hours prior. Prior to reading, fresh media (DMEM +/+) containing 471uM D-Luciferin potassium salt (Xenolight; Perkin Elmer) was added. The edge wells of the plate were filled with DMEM +/+ and the plate was sealed using a qPCR plate seal (Eppendorf) and Parafilm around the sides of the plate. Luminescence was read every 10 minutes for 48 hours using the SpectraMax I3 (Minimax 300 Imaging Cytometer; Molecular Devices), with the chamber kept at 37^{o}C. All analysis is performed using a two-way ANOVA, with a post-hoc Tukey multiple comparison test.

For infection, cells (n=6) were counted prior to a low volume infection with cell extracted WT Ad5, E4orf4- Ad5 and E1B 55K- Ad5 at an MOI of 35. The infection was allowed to progress for 15 minutes, after which the wells were supplemented with D-luciferin DMEM +/+ to a final volume of 200µL and read. For transfections, cells (n=5) were transfected with HA - E4orf4 and mutants HA-E4orf4 K88A, HA-E4orf4 F84A, HA-E4orf4 R69/70/72-75A, HA E4orf4 R81A/F84A and HA-E4orf4 R73-75A or co- transfected with CNNM WT (gift from Dr. Michel Tremblay) and HA-E4orf4 WT and class I mutants HA-E4orf4 R69/70/72-75A, HA-E4orf4 R81A/F84A and HA-E4orf4 R73-75A (Gift from Dr. Phillip Branton). The transfection proceeded in Opti-MEM for 4 hours, after which the media was changed to DMEM +/+ containing D-luciferin. Representative Western blots performed at 24 hpt by transfecting HeLa-fLUCcp cells in 6-well plates using the same ratio between DNA types and the same DNA to lipofectamine ratio as used in the 96-well plates. Samples washed with 1X PBS and immunoblotting performed as described. For interferon stimulation, IFNα1 (Sigma), IFNβ1 (Peprotech) and IFNγ (Peprotech) were added to DMEM+/+ containing D-luciferin, at 25 and 50ng/m, and used to

replace media immediately prior to reading. To confirm stimulation of cells, HeLa-fLUCcp were stimulated in a 6 well plate with either 25ng/mL or 50ng/mL of IFNα, IFNβ and IFNγ, and harvested into 1X cold PBS at 30 minutes post stimulation to perform a Western blot against STAT1 and phosphoSTAT1 (pSTAT1).

2.10 Quantitative Polymerase Chain Reaction

H1299 cells were infected with either E4orf4- or WT Ad5 and harvested at several time points after infection by scrapping cells into the supernatant, pelleting, washing with 1X PBS and pelleting to freeze. Frozen cell pellets were resuspended in Hirt extraction buffer (0.01M Tris pH 7.9, EDTA, NaCl, SDS and proteinase K) and incubated overnight at 55^{o}C. Hirt extraction using phenol/chloroform/isoamyl alcohol was used to isolate low molecular viral and host cell DNA, which was precipitated with the addition of glycogen using cold 100% ethanol (EtOH). Samples were then washed in 70% EtOH, then 100% EtOH, and resuspended in sterile water (Wisent) for storage at -20^{o}C.

Relative quantification was done using quantitative polymerase chain reaction (qPCR; BioRad CFX Connect Real Time System), to determine the Ad5 genome copy number fold change difference between the two infections. Primer set forward 5' – CTT ACC CCC AAC GAG TTT GA – 3' and reverse 5' – GGA GTA CAT GCG GTC CTT GT – 3' created by Ross et al. (2011) [100] for the hexon region of HAd DNA was used to determine Ad5 genome copy number. For the reference gene, chosen as cytochrome B on mitochondrial DNA, the primer set forward 5' – AAC TAC AAG AAC ACC AAT GAC CCC – 3' and reverse 5' – GCC GAT GTT TCA GGT TTC TGA G – 3' created by Badralmaa and Natarajan (2013)[101] was used. The qPCR used dye-based detection (iQ SYBR Green Supermix; BioRad) with an annealing temperature of 56^{o}C for both primer pairs,

and with an amplification cycle of 40 for the Ad5 hexon pair and 50 for the cytochrome B pair. The runs were performed in technical triplicate and biological triplicate, using an internal calibration standard to set the threshold consistently between plates (Eppendorf).

The fold change in DNA expression was calculated using the Livak – Schmittgen method [102]. Data is presented as linearized ΔΔCq, ($2^{-\Delta\Delta Cq}$), with WT Ad5 treated as the control and E4orf4- Ad5 as the treatment. Error is presented on linearized ΔΔCq as ± 1.0 SEM. P values were calculated on the log-base ΔCq values, comparing E4orf4- Ad5 DNA expression levels to WT Ad5 expression levels, at each timepoint using an unpaired t-test (Holm-Sidak Method).

2.11 Statistical Analysis

GraphPad Prism 8.0 was used to create figures and perform all statistical analysis. Data is presented as mean ± 1.0 SEM. Analysis performed using one way ANOVA for multiple samples, two-way ANOVA with Tukey post-hoc multiple comparison analysis for kinetic luciferase experiments or Student t-test for two sample comparison. Student t tests assumed Gaussian distribution, with the same standard deviation. P values reported using ns ($p > 0.05$), * ($p \leq 0.05$), ** ($p \leq 0.01$), *** ($p \leq 0.001$), **** ($p \leq 0.0001$).

3. Results

3.1 Characterization of the effects of extracellular magnesium alteration on Ad5 Replication

3.1.1 Magnesium depletion during Ad5 infection decreases efficiency of Ad5 replication

For this project, physiological magnesium was defined as 0.81mM, the concentration present in the DMEM used for cell culture. To determine the effect lower than physiological magnesium has on Ad5 replication, the first step was to look at the effect of magnesium depletion on the host cell. Live cell imaging was used to map the growth curve of H1299 cells when exposed to different extracellular magnesium concentrations. As shown in Figure 1A, magnesium depletion leads to a reduced rate of cell growth. From this assay, the cell specific minimum magnesium requirement was determined to be 0.0081mM, as this is the lowest concentration possible before cell growth is severely impacted. To determine which source of Mg^{2+} to use, either $MgCl_2$ or $MgSO_4$, live cell imaging was also performed under different magnesium conditions, but no significant difference was found between the two sources of magnesium. To study magnesium depletion in the context of infection, H1299 cells were maintained at their specific concentration for one week prior to infection, to reduce the amount of available magnesium in the cell. A replication assay was performed at an MOI of 5 with WT Ad5, and the media changed to have varying concentrations of magnesium. Figure 1B shows that there is a significant decrease in viral replication, correlated to the titer of the sample, when magnesium is severely depleted during infection. This suggests that magnesium plays an important role in the viral replication process.

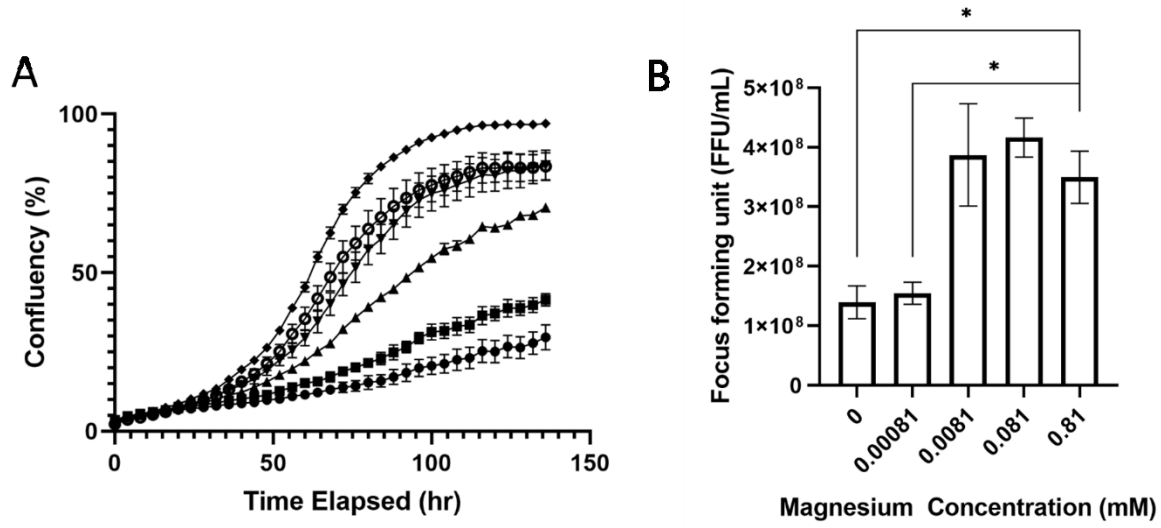

Figure 1. Depletion of magnesium during Ad5 infection

A. Live cell imaging of H1299 cells to form a growth curve, performed under different magnesium conditions: 0mM (●), 0.00081mM (■), 0.00405mM (▲), 0.0081mM (▼), 0.081mM (◆) and 0.81mM (o; physiological).
B. Replication assay for WT Ad5 infected H1299 cells under different magnesium depleted conditions. Cells maintained at 0.0081mM $MgSO_4$ for one week prior to infection. Student t-test used for two sample comparison, $p = 0.0153$ for 0mM and $p = 0.0150$ for 0.00081mM compared to physiological. Experiments performed in triplicate, presented as mean ± 1.0 SEM.

3.1.2 Magnesium supplementation during Ad5 infection does not have a significant effect on replication efficiency

Using a replication assay to compare viral production under magnesium supplementation showed no significant difference in viral replication between magnesium conditions. However, the replication assay protocol used determines the viral titer after one replication cycle. In order to determine the effect of magnesium supplementation on a long-term infection with several replication cycles, a plaque assay was performed. The plaque assay requires a monolayer of cells to be infected with a limiting number of virus particles, then overlayed with agar to limit the spread of virus to neighbouring cells only. This creates a plaque of dead cells, which can then be imaged, as seen in the representative well image, Figure 2A. The overlay contained varying amounts of magnesium, and cells were incubated for 7 to 9 days to form plaques visible to the eye, which could then be sized and counted using fluorescence microscopy. In infections using GFP-Ad5 and HEK293 cells, there was no significant difference in either mean plaque diameter or mean plaque number between the supplemented conditions, as seen in Figure 2B and C, respectively.

In order to determine if this effect is cell type dependant, HeLa cells were infected with WT Ad5 and incubated until visible plaques formed, which were then counted by eye, shown in Figure 2D. However, no increase was seen between the level of supplemented magnesium and the number of plaques formed when HeLa cells were used. In fact, it seems elevating the extracellular magnesium levels during Ad5 infection interferes with replication in HeLa cells. These experiments suggest that significantly increasing magnesium levels above physiological confers no advantage in terms of Ad5 replication.

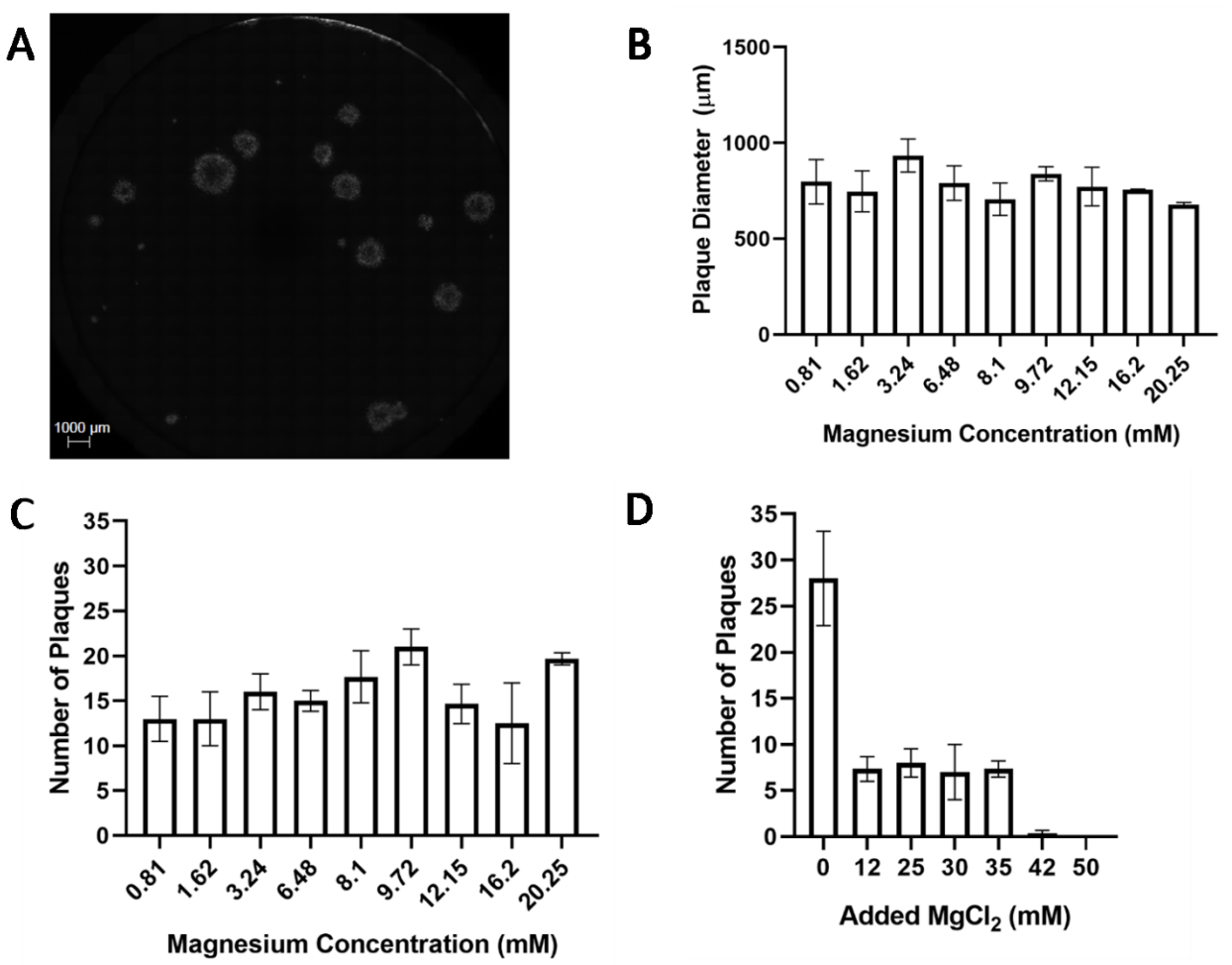

Figure 2. Supplementation of extracellular magnesium during Ad5 infection
A. Representative whole well fluorescent image of HEK293 cells infected with GFP-Ad5 and overlayed with $MgCl_2$, imaged 7 days post infection **B.** Mean plaque diameter of HEK293 infected with GFP-Ad5 **C.** Mean plaque number of HEK293 infected with GFP Ad5 **D.** Mean plaque number for HeLa infected with WT Ad5, overlayed with $MgCl_2$, counted 8 days post infection. All experiments are performed in triplicate, presented as mean ± 1.0 SEM and analyzed using one way ANOVA, no significant differences between supplemented Mg concentrations.

3.2 Characterization of E4orf4 loss on Ad5 replication and protein expression

3.2.1 E4orf4 null Ad5 infection produces higher relative genome copy number

To determine the effect E4orf4 loss has on viral DNA expression, qPCR was used to compare relative viral DNA copy number between an E4orf4- Ad5 and WT Ad5 over a time course infection. Figure 3 shows the fold change difference between E4orf4- Ad5 and WT Ad5. There is a significant difference between expression levels onwards from 12 hours post infection, as 12 hours is when viral DNA replication is occurring and viral gene expression is transitioning to the late phase. This suggests that loss of E4orf4 leads to an increase in viral genome copy number.

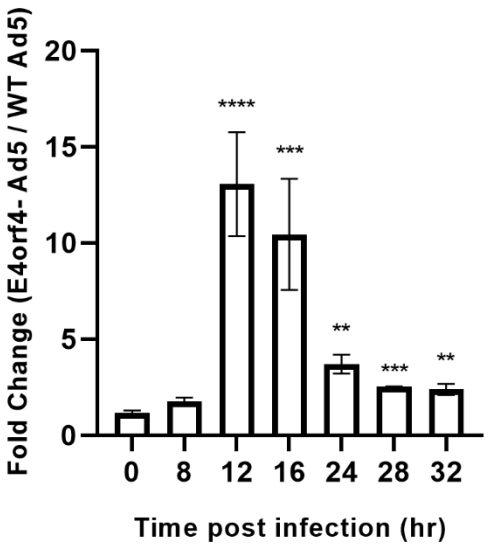

Figure 3. Determination of relative genome copy numbers during WT and E4orf4 null Ad5 infection using quantitative PCR

Fold change in expression levels of Ad5 genome from H1299 cells infected with E4orf4- Ad5 or WT Ad5 and harvested at indicated post infection timepoint. Data is presented as mean linearized fold change ($2^{-\Delta\Delta Cq}$) ± 1.0 SEM of E4orf4- Ad5 relative to WT Ad5. P values calculated on log ΔCq values using unpaired Student t-test for each time point. P values are: 12hpi p = 0.000065, 24 hpi p = 0.001072, 28 hpi p = 0.000168 and 32hpi p = 0.0304.

3.2.2 E4orf4 null Ad5 does not have higher replication efficiency compared to wild type Ad5 infection

For Ad5 to be infectious, it requires proper capsid formation and viral DNA packaging. E4orf4- Ad5 may have higher viral DNA copy numbers, but to determine if this has any effect on its ability to form infectious particles, a replication assay was used to look at differences in viral titer, as presented in Figure 4. No significant difference is seen between E4orf4- Ad5 and WT Ad5 conditions, however the trend of the calculated titer indicates that E4orf4- Ad5 undergoes a less efficient replication cycle when compared to WT Ad5.

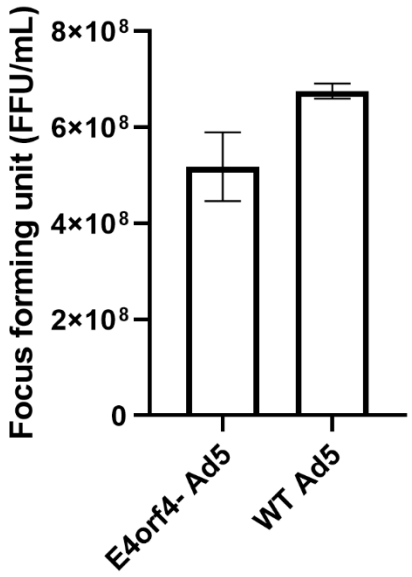

Figure 4. Comparison of WT and E4orf4- Ad5 viral titers using a replication assay
Replication assay comparing E4orf4- Ad5 to WT Ad5 infection, no significant difference seen between conditions. Grubbs outlier test performed on E4orf4- Ad5 infection replicates to determine if replicate values contain an outlier, however all fall within a 95% confidence interval. Data presented as mean ± 1.0 SEM for n = 3 replicates.

3.2.3 E4orf4 null Ad5 has higher levels of early protein expression compared to wildtype Ad5

To characterize the effect that viral E4orf4 has on viral protein expression, time course infections were completed in H1299 cells at an MOI of 5, for a period of 72 hours. The infection was performed using E4orf4- Ad5 and WT Ad5, to compare protein expression. The infected samples were then analyzed using Western blots. Figure 5 A shows that loss of E4orf4 causes an increase in early viral protein expression, using E1A and E4orf6 as representative proteins, as well as a decrease in late viral protein expression, represented by Ad5 viral capsid proteins.

3.2.4 Magnesium depletion alters early viral protein expression

Magnesium depletion was found to impact the replication efficiency of WT Ad5 and to further investigate the importance of magnesium for Ad5 replication, protein expression of E4orf4 null Ad5 and WT Ad5 was completed under less than physiological conditions, as seen in Figure 5B and quantified using a Western Blot to determine the intensity of the respective protein band, normalized to the intensity of the total lane protein (TLP) as shown in Figure 5 C. Under physiological conditions, expression is lower than under depleted conditions, suggesting that magnesium depletion alters viral gene expression and significantly increases early viral protein expression, specifically E1A and E4orf6. For viral capsid expression, magnesium depletion had no significant impact.

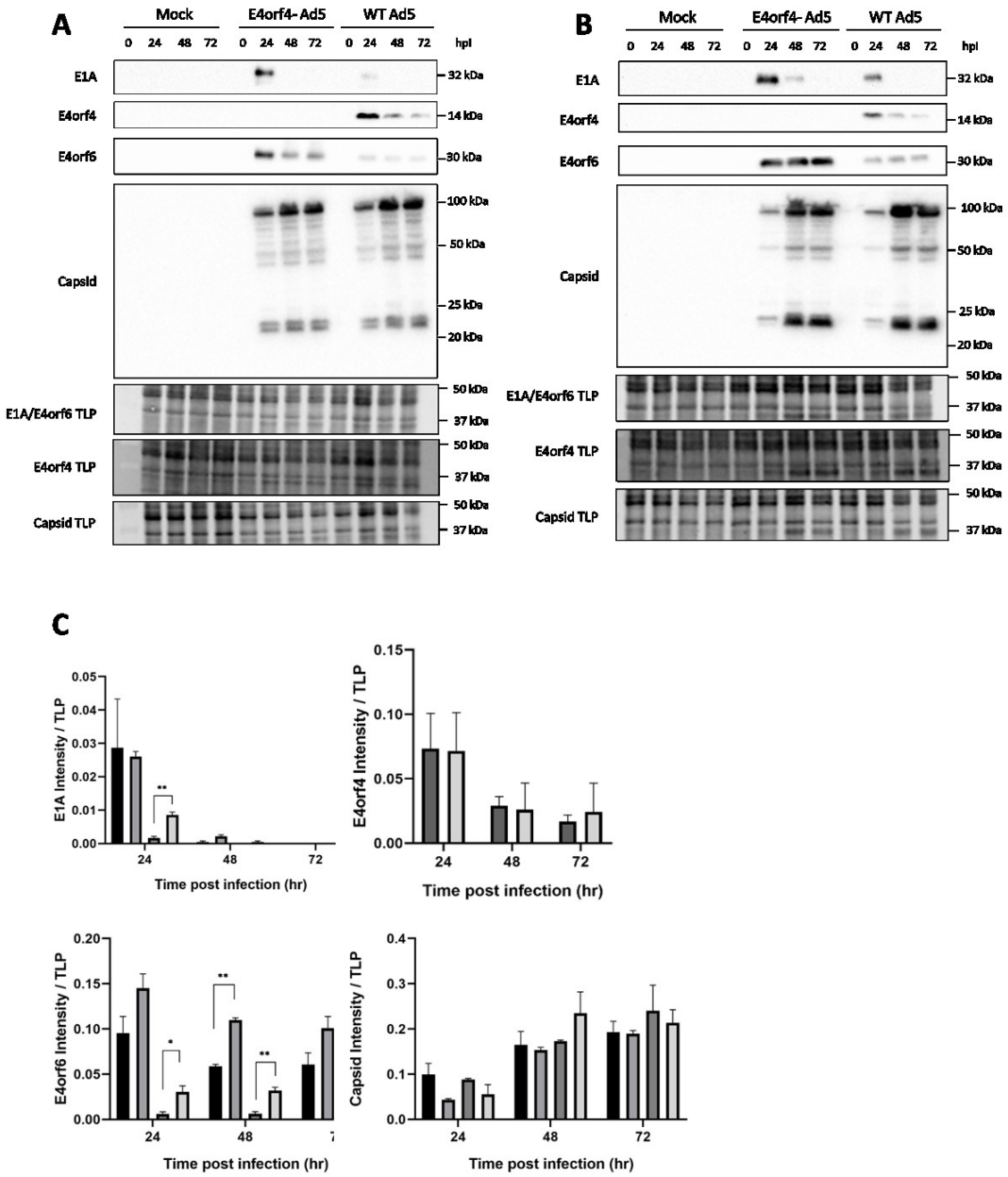

Figure 5. Protein expression of WT and E4orf4- Ad5 infection in physiological and lower than physiological magnesium conditions

A. Ad5 protein expression under physiological Mg infection (0.81mM Mg in DMEM, 10% FBS). Cells infected with either E4orf4- Ad5 or WT Ad5 at an MOI of 5 and harvested at time points indicated. **B.** Ad5 protein expression under low Mg conditions – no added magnesium (Mg free DMEM, 5% dialyzed FBS). Cells infected with either E4orf4- Ad5 or WT Ad5 at an MOI of 5 and harvested at time points indicated. **C.** Quantified protein expression levels for physiological E4orf4- Ad5 infection (black), low E4orf4- Ad5 infection (grey), physiological WT Ad5 infection (dark grey) and low WT Ad5 infection (light grey), calculated by determining band intensity and normalizing to the intensity of the total lane protein (TLP). Data presented as mean ± 1.0 SEM of triplicate infections, with p values calculated using Student's t-test for comparison between Mg levels for each infection type. For E1A protein WT infection comparison, at 24 hpi $p = 0.001956$, for E4orf6 protein E4orf4- Ad5 infection $p = 0.000102$ at 48 hpi, and for WT Ad5 infection 24hpi $p = 0.027728$, 48hpi $p = 0.003475$ and 72hpi $p = 0.000658$.

3.3 Determination of the role E4orf4 has on intracellular Mg during infection

3.3.1 Loss of E4orf4 does not have a significant effect on intracellular magnesium level alteration during infection

To investigate the changes in intracellular magnesium over the duration of a synchronous infection time course, HeLa cells that stably express the magnesium sensitive UTR of PRL2 linked to destabilized firefly luciferase were used as a reporter cell line. Decreases in intracellular magnesium levels lead to an increase in luciferase expression and therefore an increase in the reported luminescence. These cells were infected with WT Ad5, E4orf4- Ad5 and an E1B55K- Ad5 and the infection was allowed to progress for 48 hours, with kinetic luminescence readings being recorded every 10 minutes, as shown in Figure 6. The E1B55K- Ad5 was used to determine if the effects seen were due to changes in intracellular magnesium, or if they were due to decreased expression of luciferase, which may occur as host cell shutoff begins. Since the trend of E1B55K- Ad5 kinetic luminescence matches that of WT Ad5, this suggests that the effects seen are due to alterations in the intracellular magnesium levels in the infected cells. For all virus types, there is an increase in luminescence during early infection, suggesting a decrease in intracellular magnesium levels. At around 14 hours post infection, which may correlate with the early to late gene expression transition, there is a decrease in luminescence, suggesting an increase in intracellular magnesium is occurring. Comparing WT Ad5 and E4orf4- Ad5, there is no significant difference in luminescence over the duration of the infection time course, suggesting that the loss of E4orf4 in the context of infection does not impact the way magnesium is used by the virus and host cell.

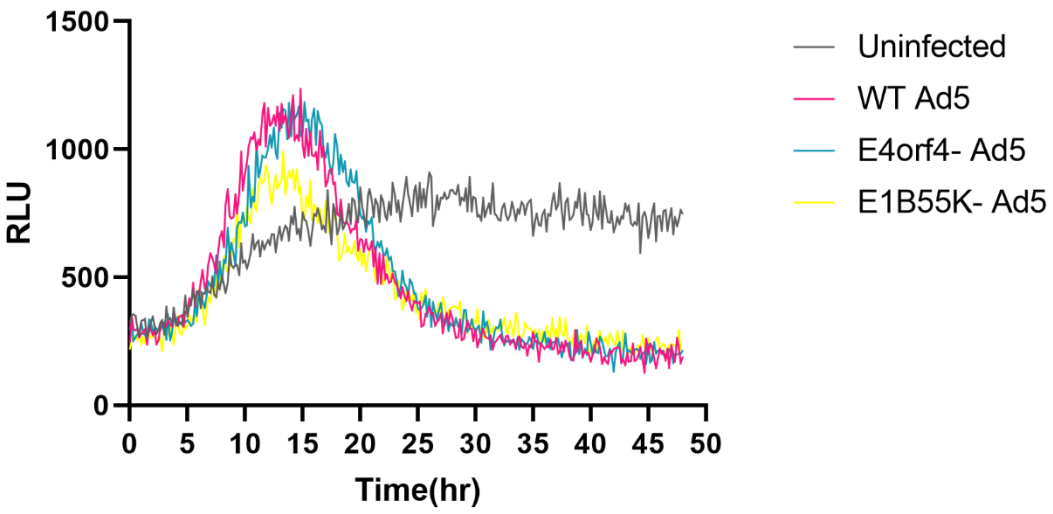

Figure 6. Infection of magnesium sensitive reporter cell line using WT, E4orf4 null and E1B55K null Ad5
Infection of HeLa-fLUCcp reporter cells with WT Ad5 (magenta), E4orf4- Ad5 (cyan) and E1B55K- Ad5 (yellow) compared to uninfected cells (black) over a time period of 48 hours, starting one hour post infection, with imaging every 10 minutes to determine luminescence output (RLU). Analysis performed using two-way ANOVA for n = 6 replicates, with a $p < 0.0001$ between mock and infected cells.

3.3.2 Expression of E4orf4 increases the total cellular magnesium concentration

To look at the effect of E4orf4 expression on total cellular magnesium outside the context of infection, cells were transfected with HA-E4orf4 or a class I mutant HA-E4orf4 R81A/F84A that lacks the ability to bind to PP2A, the location of this mutation in E4orf4 shown in Figure 7A. The total level of magnesium in these transfected samples were measured using ICP-OES, as seen in Figure 7B. When expressed alone, E4orf4 can significantly increase the total cellular magnesium concentration when compared to its non-functional mutant, suggesting that outside the context of infection E4orf4 does have the ability to alter total magnesium levels.

3.3.3 Expression of E4orf4 in magnesium sensitive reporter cell line does not significantly increase the intracellular magnesium concentration

To further determine the role E4orf4 alone plays in altering the intracellular magnesium concentration, HA-E4orf4 WT and class I mutants HA-E4orf4 R69/70/72-75, HA-E4orf4 R81A/F84A and HA-E4orf4 R73-75A, seen in Figure 7A, were transfected into the reporter cell line, as shown in Figure 7C. Compared to the empty vector control, there was no overall significant difference between transfection conditions when performing post-hoc comparisons. While there is significance at some time points, the next reading is reported as not significant and should be taken into account as there is variability between readings. At the beginning of luminescence reporting, the trend of transfected samples compared to the empty vector control seems to show an increase, which correlates to a decrease in intracellular magnesium levels. Additionally, the HA-E4orf4 R69/70/72-75 mutant seems to continue to experience a depletion in intracellular magnesium. Overall, no significant increase in intracellular magnesium was seen using this reporter cell line during transfection with HA-E4orf4 WT, and no loss of

intracellular magnesium alteration was seen with HA-E4orf4 class I mutants, suggesting that E4orf4 alone may not be enough to alter intracellular magnesium levels.

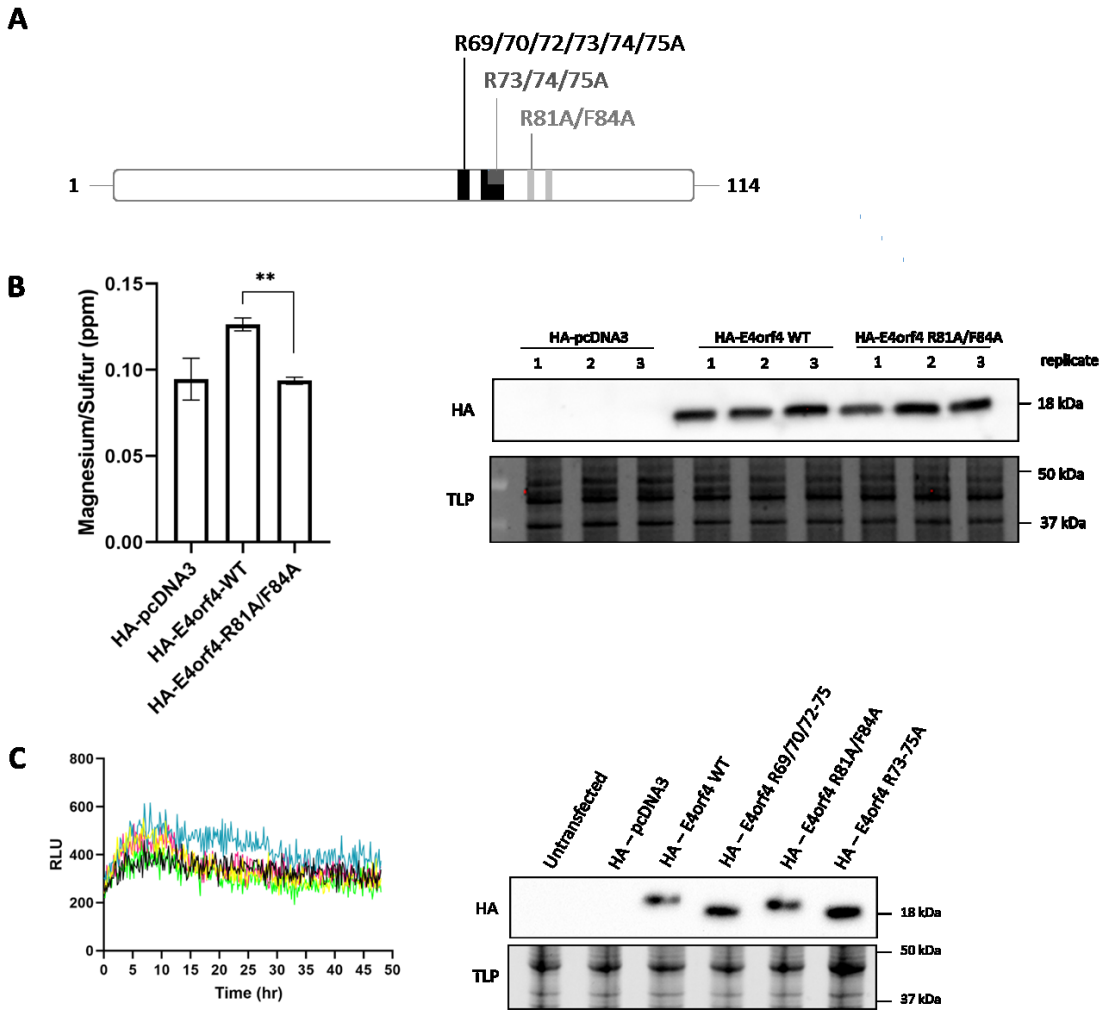

Figure 7. Role of E4orf4 in alterations to total and intracellular magnesium concentrations
A. Illustration of the E4orf4 Class I mutations E4orf4 R69/70/72/73/74/75A (black), E4orf4 R73/74/75A (dark grey) and E4orf4 R81A/F84A (light grey). **B.** Measurement of total cellular Mg using ICP-OES in H1299 cells transfected with HA-E4orf4 WT or HA-E4orf4 R81A/F84A mutant at 48 hours post transfection, estimated transfection efficiency of 70 – 80% using EGFP at 24hpt. Experiment performed in triplicate, with data presented as mean ± 1.0 SEM and representative Western blot presented. Student's t-test used to compare HA-E4orf4 WT and HA-E4orf4 R81A/F84A, with a significance of p = 0.001603. **C.** Measurement of intracellular magnesium concentrations using magnesium sensitive HeLa-fLUCcp reporter cell line using an n = 6, reported as mean value with representative Western blot. Cells transfected with empty vector HA-pcDNA3 (black), HA-E4orf4 WT (yellow), HA-E4orf4 R69/70/72-75A (cyan), HA-E4orf4 R81A/F84A (magenta) and HA-E4orf4 R73-75A (green), estimated transfection efficiency of >90% using EGFP at 24hpt. Two way ANOVA used to determine significance, $p < 0.0001$ with Tukey post-hoc analysis to determine time points of significance, finding that significance is not constant with subsequent time points.

3.3.4 Stimulation with type I and II interferon may lead to alterations in intracellular magnesium levels when detected with magnesium sensitive reporter cell line

Interferon is expressed as part of the cellular-antiviral response, and to determine the effect IFN stimulation has on intracellular magnesium levels, cells were stimulated using type I IFNα and IFNβ, as well as type II IFNγ. As seen in Figure 8A, it appears IFNα stimulation does not alter intracellular magnesium in the cell, as the trend for this method of stimulation follows the same trend as the unstimulated cells. Looking at the Western blot for phospho-STAT1 expression, Figure 8D, there does not seem to be a large increase in pSTAT1 upon IFNα stimulation, suggesting that this stimulation was not very effective. This could be why no significant difference was seen between the unstimulated and IFNα stimulated conditions. For IFNβ and IFNγ as shown in Figure 8B and C respectively, the concentration of IFN used to stimulate the cells is sufficient, as either concentration shows the same trend for intracellular magnesium sensing reporter cell line, as well as similar activation of STAT1 as shown by phospho-STAT1 expression levels. There is a significant difference between the stimulated and unstimulated cells starting around 18 hours post stimulation for IFNβ and IFNγ when comparing each condition using Tukey multiple comparison test post two-way ANOVA, however this difference in luminescence may be due to cell death and lack of luciferase expression rather than intracellular magnesium alterations alone. This result suggests that stimulation with either type I or type II interferon may lead to alterations in intracellular magnesium concentrations, but further optimization is needed to determine if apoptosis is interfering with the reporter cell line output.

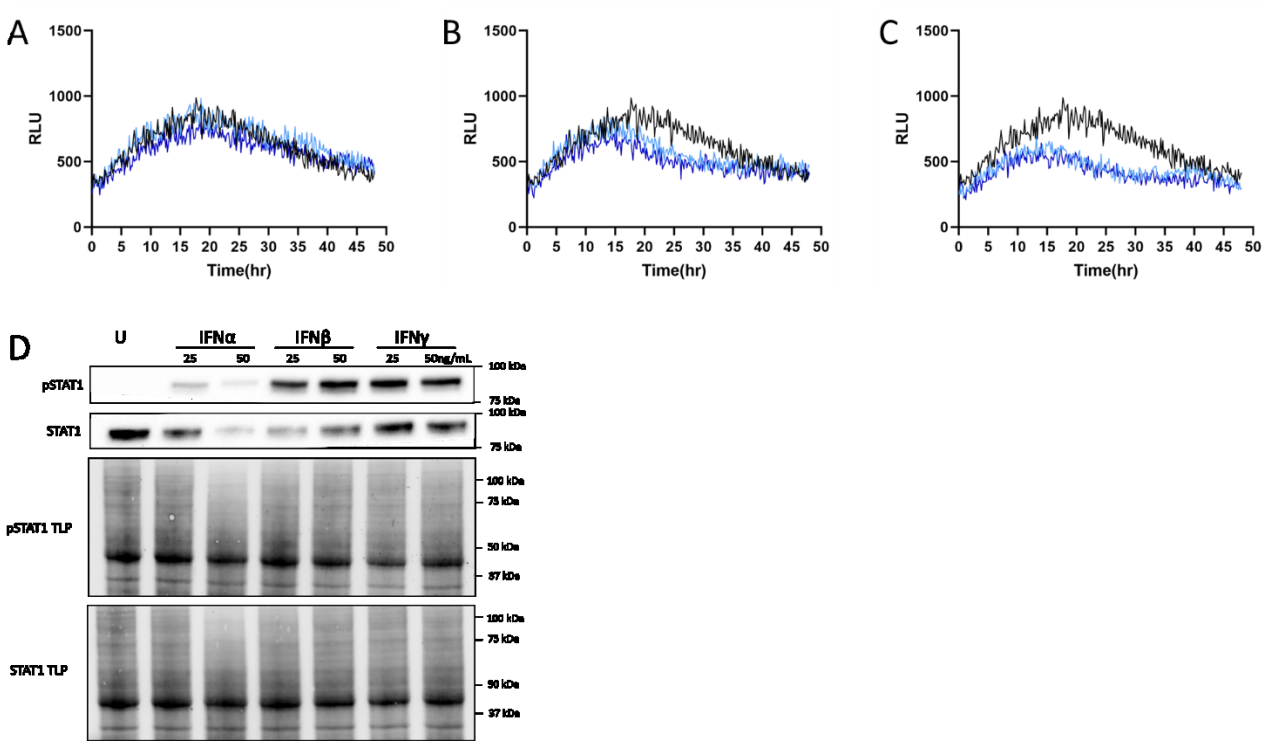

Figure 8. Stimulation of magnesium sensitive reporter cell line with type I and type II interferon
A. Addition of 25ng/mL IFNα (light blue) or 50ng/mL IFNα (dark blue) to HeLa-fLUCcp cells (black). **B.** Addition of 25ng/mL IFNβ (light blue) or 50ng/mL IFNβ (dark blue) to HeLa-fLUCcp cells (black). **C.** Addition of 25ng/mL IFNγ (light blue) or 50ng/mL IFNγ (dark blue) to HeLa-fLUCcp cells (black) with luminescence readings every 10 minutes for 48 hours for all samples. Analysis performed with n = 5 replicates per condition, with data presented as the mean. Two-way ANOVA used to determine significance, $p < 0.0001$ with Tukey post-hoc analysis to determine time points of significance, finding that significance is not constant with subsequent time points. **D.** Representative Western Blot of HeLa-fLUCcp cells simulated with 25ng/mL or 50ng/mL of IFN 30 minutes prior to harvest on ice.

3.4 Investigation of the importance of CNNM3 for magnesium alteration by E4orf4-PP2A

3.4.1 Co-transfection of CNNM3 with E4orf4 WT does not lead to alterations in intracellular magnesium using magnesium sensitive reporter cell line

Ad5 E4orf4 has been found to interact with the potential magnesium homeostasis complex CNNM3/PRL2, so to investigate if this interaction has an effect on intracellular magnesium levels, CNNM3 was co-transfected with HA-E4orf4 WT and class I mutants in the magnesium sensitive HeLa reporter cell line. Figure 9 shows that transfection of E4orf4 WT alone, or co-transfection with CNNM3 does not significantly alter the levels of intracellular magnesium compared to the empty vector control, or to the respective E4orf4 type when transfected alone. The class I mutants E4orf4 R81A/F84A and E4orf4 R73-75A show no alterations in intracellular magnesium, as expected since the ability of E4orf4 to target the CNNM3/PRL2 complex using PP2A is lost. E4orf4 class I mutant R69/70/72-75A does show alterations in intracellular magnesium levels, a decrease in intracellular magnesium is reported with and without co-expression of CNNM3. This mutant also lacks the ability to bind PP2A, so the mechanism of action by which intracellular magnesium is being altered is unclear, as well as if this alteration is biologically significant.

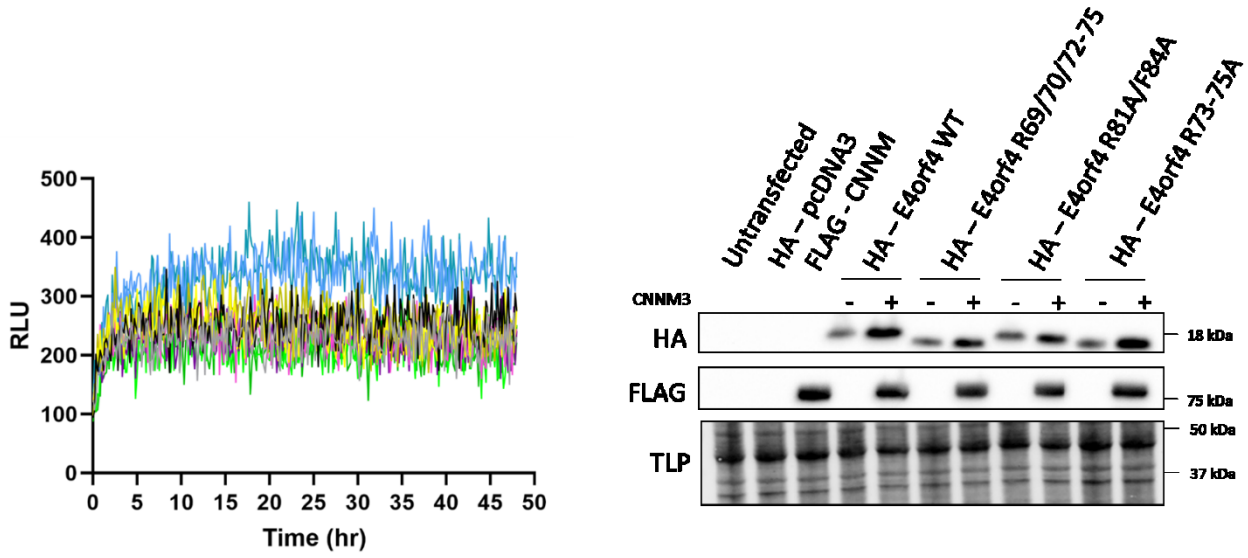

Figure 9. Co-transfection of HA – E4orf4 WT and class I mutants with CNNM3 in magnesium sensitive reporter cell line

Measurement of intracellular magnesium concentration of magnesium sensitive HeLa-fLUCcp reporter cell line transfected with HA-pcDNA3 (gray), CNNM alone (black), HA-E4orf4 WT (yellow), HA-E4orf4 WT + CNNM3 (dark yellow), HA-E4orf4 R69/70/72-75A (cyan), HA-E4orf4 R69/70/72-75A + CNNM3 (dark cyan), HA-E4orf4 R81A/F84A (magenta), HA-E4orf4 R81A/F84A + CNNM3 (dark magenta), HA-E4orf4 R73-75A (green) and HA-E4orf4 R73-75A + CNNM3 (dark green). Data presented as mean of n = 5 samples, two-way ANOVA $p < 0.0001$ with Tukey post-hoc analysis to determine time points of significance, finding that significance is not constant with subsequent time points. Data presented with representative Western blot at 24 hours post transfection.

4. Discussion

4.1 Characterizing the effects of extracellular magnesium alteration on Ad5 replication

Past experiments looking at the effect of magnesium on viral replication have postulated that increased magnesium is beneficial for the virus during infection, and thus finding a complex involved in magnesium homeostasis as a potential target for a viral protein is very interesting [29,73]. In order to replicate, viruses require host cell machinery, and anything that could benefit the host cell may also benefit the virus. Since magnesium plays a role in DNA and protein synthesis, both of which are required during infection, increasing the intracellular magnesium levels may confer an advantage for the virus. In order to characterize the effect of magnesium on the viral replication process, magnesium depletion was first studied. While this may not be clinically relevant, depleting extracellular magnesium *in vitro* shows the importance of magnesium for viral replication as low levels of magnesium decreases the efficiency at which Ad5 can replicate. However, in order to study viral replication at lower than physiological levels, the host cells had to be maintained at a lower level of magnesium and then incubated in magnesium free media during the 28-hour infection period. In addition, to minimize the amount of magnesium present, the media used to maintain and infect the cells contained 5% dialyzed FBS compared to the 10% of normal FBS used to maintain cells in culture, which may alter the behaviour of the maintained cells. The duration of infection corresponds to approximately one cellular cycle in uninfected cells, however differences in viral replication observed between the no added magnesium and physiological levels may be in part due to cell growth being negatively affected by magnesium depletion for the no added magnesium and 0.00081mM conditions. There is a strong effect seen starting at 0.00081mM in terms of cell

growth impairment and this is where the viral titer begins to significantly decrease when compared to the physiological magnesium titer. This decrease in titer may potentially be due to insufficient magnesium availability for normal cellular functions, rather than due to the effect of magnesium on the viral replication process alone.

When studying the effects of extracellular magnesium supplementation on viral replication, Williams (1970) [73] had suggested that increased magnesium lead to an increase in the rate of Ad5 release, demonstrating this result using a plaque assay of HeLa cells infected with wild type Ad5, finding that an increase in extracellular magnesium lead to larger plaques that appeared sooner [73]. This result was unable to be replicated, both in HEK293 and in HeLa cell lines. The cell lines chosen for this portion of the project may not be optimal as neither HEK293 nor HeLa are respiratory epithelial cell lines, which are the main target of Ad5 for infection [103]. In addition, cancer cell lines like HeLa have altered pathways in response to changes in metabolic need, so the lack of response to increased magnesium seen in these cell lines during infection may vary compared to infections in primary cell lines [77,83]. The WT Ad5 used for this project is missing a portion of the E3 region, which assists in mitigating the immune response by the host cell and helps to encourage apoptosis during late infection [87]. This portion of the genome may be involved in the magnesium dependent effect seen by Williams (1970) [73], which may explain why a significant trend with increasing magnesium was not seen using a true WT Ad5.

4.2 Characterization of E4orf4 loss on Ad5 replication and protein expression

Comparing the relative genome copy number of E4orf4 null and wildtype Ad5 infections shows E4orf4 null Ad5 infection produces a significantly higher copy number. However, this

does not correspond to an increase in replication efficiency, when the titer of infections viral particles was measured using a replication assay. Additionally, CPE visually appears to be more severe for a WT Ad5 infection, when compared to an E4orf4- Ad5 infection at the same time point. Loss of E4orf4 means the transition from early to late gene expression is altered, as more early viral proteins are produced in an E4orf4 null infection. These proteins are responsible for preparing the host cell for viral DNA synthesis, which may help to explain why there are higher genome copy numbers in the E4orf4 null Ad5 infection samples. Late viral protein expression is not significantly different in a wild type infection compared to an E4orf4 null infection.

Looking at differences in viral protein expression under varying magnesium conditions, significant effects are only seen for early proteins, suggesting that magnesium is required early in infection rather than during the later phases of infection. This is in contrast to what Williams (1970)[73] had seen, as he postulated that magnesium is required for viral release, the last stage in viral infection. Additionally, magnesium played a more significant role when comparing protein expression under physiological and lower than physiological conditions for wild type Ad5 infection. This is interesting as early viral protein expression is lower compared to E4orf4 null Ad5 infection, yet there is a stronger response to magnesium. This experiment should be repeated in a cell line where infection shows a clearer dependence on magnesium, if possible.

4.3 Determination of the role E4orf4 has on intracellular Mg during infection

The HeLa-fLUCcp cell line was created by the lab of Dr.Tremblay, by linking the expression of destabilized firefly luciferase to the expression of the uORF of PRL2, which is thought to be magnesium sensitive. When magnesium levels in the cell decrease, the translation of this UTR increases, thus increasing the expression of luciferase. Destabilized

firefly luciferase is used as it has a shorter half-life and will not accumulate to such levels that the wildtype protein would, allowing for changes in expression to be seen [99]. The benefit to using this cell line is that luciferase expression is endogenous, and does not require additional transfection and controls such as renilla. As well, most commercially available magnesium probes are not entirely specific to magnesium as alterations in other divalent ions such as calcium can affect the output of the probe [104]. However, this cell line will require further optimization and validation in order to determine the pool of intracellular magnesium that is being sensed, as this has an impact on interpretation of the results. Linking the luminescence output of the cells to the specific intracellular magnesium concentration is another potential direction for this assay, and this can be done by creating a standard curve of magnesium concentrations using an ionophore to artificially alter the intracellular magnesium concentrations [105]. To confirm the concentrations, ICP-OES can be used to measure total cellular magnesium of a control set of samples and compare this to the samples where magnesium levels are altered. For this project, the reporter cell line was used to give an indication of overall behaviour of cells either infected or transfected. A drawback to this assay was the method used for capturing luminescence values requires cells to be incubated in non-ideal conditions, mainly atmospheric CO_2 levels, which could also impact the results obtained. Additionally, transfection is harsh on the cells, and a significant portion are dead by 48 hours post transfection, in some wells more than others. Biological replicates are used, and experiments are repeated to confirm results, but it is difficult to replicate results seen. Transfections are optimized in 6-well plates prior to running the reporter cell line kinetic luciferase assay, in order to try and have even expression of WT and mutant proteins. For the

96-well transfections, the same DNA ratios are used, but Western blots cannot be used to verify, making it difficult to draw conclusions. These kinetic luciferase experiments should be used to help determine important time points, and at these time points, end point luciferase assays should be performed at time points of interest to confirm the behaviour seen with the kinetic luciferase and ensure significance between sample conditions.

For HeLa-fLUCcp cells infected with Ad5, the trend seen indicates that the loss of E4orf4 during infection is not required to cause the altered magnesium concentrations observed. While there does seem to be a slight shift in timing, the luminescence output of E4orf4- Ad5 matches that of WT Ad5. Around 14 hours post infection there is a shift from a decrease in intracellular magnesium to an increase, corresponding to what was seen using ICP (preliminary experiment - not shown), that at around 12 hours post infection, the level of intracellular magnesium was seen to increase in infected cells, when compared to uninfected cells. However, no initial decrease was seen by ICP, suggesting that changes in the cell are happening in the free pool of magnesium, which is why further optimization of this assay is needed to determine which pool is being sensed. At around 14 hours post infection, at an MOI of 35, viral DNA replication should be well underway, so it would be interesting to confirm by Western blot that this change in magnesium corresponds to the onset of viral DNA replication, as this may help to explain the initial depletion in magnesium as magnesium is an important cofactor for DNA synthesis. When comparing protein expression between physiological and lower than physiological infections, it seems magnesium is required for early infection, also explaining why there is an initial depletion of magnesium. E4orf4 is present at the time of viral DNA replication, yet since the E4orf4- infection still shows alterations in magnesium, this suggests that E4orf4

may not be vital to altering intracellular magnesium and that further testing is needed. Endpoint luciferase assays should be performed to validate the trend seen, with specific focus around 14 hours post infection.

Infection with Ad5 causes numerous changes in the behavior of the host cell: protein expression is preferential for viral proteins, the cell cycle shifts to S phase, apoptosis pathways are blocked, and immune pathways are activated in response to the virus [5]. In order to study the effect that E4orf4 alone, without the presence of other viral proteins that may alter its function, and without the massive changes to the host cell seen during infection, E4orf4 was transfected into H1299 cells to determine the effect of E4orf4 on intracellular magnesium, compared to a class I E4orf4 mutant, HA-E4orf4 R81A/F84A. This mutant was chosen as it acts as a class I, that is it lacks the ability to properly bind to PP2A, in both H1299 and HeLa cells [30]. The total cellular magnesium levels were tested using ICP, showing that HA-E4orf4 WT does cause an increase in magnesium levels when compared to the mutant, suggesting that functional E4orf4 is required. However, ICP-OES can only show changes in total magnesium, which is the net magnesium in the cell, either gained by influx or lost by efflux, it cannot show changes in the pool of free magnesium. To understand better what is happening to intracellular magnesium levels, the reporter cell line assay was transfected with HA-E4orf4 WT and class I mutants. However, no clear conclusions could be drawn, as analysis of the kinetic luciferase assay showed no significant differences between transfection conditions. In addition, early in reporting, which corresponds to 4 hours post transfection and onward, there seems to be a slight elevation in luminescence, which corresponds to a decrease in intracellular magnesium, going against the hypothesis that E4orf4 is required to increase intracellular magnesium levels.

To determine if this alteration is meaningful, endpoint luciferase should be used to understand what is occurring. It seems that while E4orf4 can alter total cellular magnesium, either by increasing influx or blocking efflux, it cannot alter the way magnesium is processed inside the cell, and what pools of magnesium are available to be sensed by the assay. Further optimization is needed to make any conclusions about the significance E4orf4 has on alterations to intracellular magnesium levels.

Infection rapidly activates the host cell immune response, and this response may also be playing a role in intracellular magnesium alteration. Type I IFN response pathways are commonly produced by the host cell during infection, and type II IFN response pathways are usually in response to infection by immune cells [80]. To determine the role that both pathways may play, the reporter cell line was stimulated using two different concentrations to ensure a response, which was validated by looking at changes in STAT1 phosphorylation, which occurs as part of the IFN pathway for both types. IFNα was not observed to increase phosphorylation of STAT1, nor alter intracellular magnesium levels as the trend for IFNα stimulated cells showed no difference compared to the trend of unstimulated cells. This requires further optimization as HeLa cells are sensitive to IFNα stimulation [106]. For IFNβ and IFNγ, both concentrations of IFN used caused an increase in pSTAT1 and a change in the trend of intracellular magnesium levels. However, IFN can lead to cell death, so to determine if the effects seen are due to intracellular magnesium changes alone, a viability or apoptosis assay should be performed. While these results are inconclusive as further optimization and viability assays are required, as a next step it would be interesting to check levels of magnesium homeostasis proteins such as TRPM7, CNNM3 and PRL2 in cells stimulated with IFN. Cancer cells experience changes in their

metabolism pathways, as well as different gene regulation. The cGAS-STING pathway, which is involved in the host cell immune response, has been shown to be impaired in HeLa cells [107]. Additionally, PRL has been shown to be upregulated in cancer cells, so repeating these experiments in different cell lines could give a better indication of what is happening to intracellular magnesium during infection. Finally, a future direction could be to serum starve the cells prior to interferon stimulation, as this will help to align the cell cycles, mimicking what happens in infection where Ad5 protein E1A pushes the host cell into S phase to begin viral DNA replication.

4.4 Investigation of the importance of CNNM3 for magnesium alteration by E4orf4-PP2A

In order to better understand the importance of Ad5 E4orf4 targeting the CNNM/PRL complex during infection, co-transfection of E4orf4 was done with CNNM3 in the magnesium sensitive reporter cell line. When E4orf4 WT is expressed, either alone or with CNNM3, the hypothesis is that intracellular magnesium should increase, as E4orf4 targets CNNM3. However, this effect was not seen, reported magnesium levels matched that of the empty vector, suggesting that E4orf4 alone is not enough for the increase seen in total levels of magnesium. Transfection with the E4orf4 class I mutants was used to determine if loss of PP2A binding led to loss of intracellular magnesium alteration, as these samples should have the same levels of magnesium as the empty vector controls. E4orf4 mutant R69/70/72-75A had higher reported luminescence, correlating to lower levels of intracellular magnesium in comparison to the empty vector control. This trend is interesting, as the region of E4orf4 mutated for the class I mutants contains an arginine-rich motif that may be important for localization of E4orf4,

specifically arginine resides 66-75 [108]. Out of all the mutants used, the E4orf4 R69/70/72-75 contains the most mutations, and when looking at the size of the protein via Western blot, presents as a lower band compared to E4orf4 WT. For the class I mutant E4orf4, having even protein expression was difficult, even after adjusting the transfected DNA amounts to compensate for lower protein expression. As the transfection DNA amounts were optimized in 6-well plates, it is difficult to verify protein expression in the 96-well plates used for the kinetic luciferase assay. Further optimization is again required, as transfection is harsh on the reporter cell line, and cell death may be interfering with reported luminescence values over time.

4.5 Conclusions

Magnesium plays an important role for the host cell, and having a viral protein specifically interacting with a protein complex involved in magnesium homeostasis suggests that magnesium is important for the virus infection cycle too, however the role of magnesium in viral infection is still unclear. Further experimentation is required to determine if the lack of response to additional extracellular magnesium seen is cell line dependent. If the increase in total cellular magnesium seen in infected cells is biologically significant, adding extracellular magnesium in excess, at levels not physiologically relevant, may be impeding the viral replication process. It is also difficult to draw conclusions based on the kinetic luciferase assay experiments, these experiments should be used as a way to understand overall trends between samples. To continue these experiments, end point luciferase assays should be performed at time points of interest. Validation of the magnesium sensitive reporter cell line is needed, as it is important to understand the biological significance behind the alterations to intracellular magnesium seen.

Interestingly, Ad5 is not the only virus to potentially target CNNM3, Li et al. (2021) performed a proteomic study of the interaction of SARS-coV-2 with the host cell, finding that accessory protein orf8 interacts with CNNM3 [109]. Determining the importance of CNNM3 dephosphorylation by the E4orf4-PP2A complex could help elucidate the importance of magnesium during infection, a promising direction not just for adenovirus but other virus families as well.

5. References

1. Rowe, W. P., Huebner, R. J., Gilmore, L. K., Parrott, R. H. & Ward, T. G. Isolation of a Cytopathogenic Agent from Human Adenoids Undergoing Spontaneous Degeneration in Tissue Culture. *Proc. Soc. Exp. Biol. Med.* **84**, 570–573 (1953).
2. Mennechet, F. J. D. *et al.* A review of 65 years of human adenovirus seroprevalence. *Expert Rev. Vaccines* **18**, 597–613 (2019).
3. Russell, W. C. Adenoviruses: update on structure and function. *J. Gen. Virol.* **90**, 1–20 (2009).
4. Martin-Fernandez, M. *et al.* Adenovirus Type-5 Entry and Disassembly Followed in Living Cells by FRET, Fluorescence Anisotropy, and FLIM. *Biophys. J.* **87**, 1316–1327 (2004).
5. Seth, P. *Adenoviruses: Basic Biology to Gene Therapy*. (R. G. Landes Company, 1999).
6. Marcellus, R. C. *et al.* Adenovirus Type 5 Early Region 4 Is Responsible for E1A-Induced p53-Independent Apoptosis. *J Virol* **70**, 9 (1996).
7. Moran, E. Mammalian cell growth controls reflected through protein interactions with the adenovirus E1A gene products. *Semin. Virol.* **5**, 327–340 (1994).
8. Querido, E. *et al.* Regulation of p53 levels by the E1B 55-kilodalton protein and E4orf6 in adenovirus-infected cells. *J. Virol.* **71**, 3788–3798 (1997).
9. Hoeben, R. C. & Uil, T. G. Adenovirus DNA Replication. *Cold Spring Harb. Perspect. Biol.* **5**, a013003 (2013).
10. Leppard, K. N. E4 gene function in adenovirus, adenovirus vector and adeno-associated virus infections. *J. Gen. Virol.* **78**, 2131–2138 (1997).

11. Schwartz, R. A. *et al.* Distinct Requirements of Adenovirus E1b55K Protein for Degradation of Cellular Substrates. *J. Virol.* **82**, 9043–9055 (2008).
12. Babiss, L. E. & Ginsberg, H. S. Adenovirus type 5 early region 1b gene product is required for efficient shutoff of host protein synthesis. *J. Virol.* **50**, 202–212 (1984).
13. Dallaire, F. *et al.* The Human Adenovirus Type 5 E4orf6/E1B55K E3 Ubiquitin Ligase Complex Can Mimic E1A Effects on E2F. *mSphere* **1**, (2016).
14. Huang, W. & Flint, S. J. The Tripartite Leader Sequence of Subgroup C Adenovirus Major Late mRNAs Can Increase the Efficiency of mRNA Export. *J. Virol.* **72**, 225–235 (1998).
15. Leppard, K. N. Regulated RNA Processing and RNA Transport during Adenovirus Infection. *Semin. Virol.* **8**, 301–307 (1998).
16. Gros, A. & Guedan, S. Adenovirus Release from the Infected Cell as a Key Factor for Adenovirus Oncolysis. *Open Gene Ther. J.* **3**, 24–30 (2010).
17. Groitl, P. & Dobner, T. Construction of Adenovirus Type 5 Early Region 1 and 4 Virus Mutants. in *Adenovirus Methods and Protocols: Volume 1: Adenoviruses, Ad Vectors, Quantitation, and Animal Models* (eds. Wold, W. S. M. & Tollefson, A. E.) 29–39 (Humana Press, 2007).
18. Sugarman, B. J., Hutchins, B. M., McAllister, D. L., Lu, F. & Thomas, K. B. The Complete Nucleic Acid Sequnce of the Adenovirus Type 5 Reference Material (ARM) Genome. *Bioprocess J* **2**, 27–33 (2003).
19. Miron, M.-J. *et al.* Localization and Importance of the Adenovirus E4orf4 Protein during Lytic Infection. *J. Virol.* **83**, 1689–1699 (2009).

20. Kindsmüller, K. *et al.* Intranuclear targeting and nuclear export of the adenovirus E1B-55K protein are regulated by SUMO1 conjugation. *Proc. Natl. Acad. Sci.* **104**, 6684–6689 (2007).
21. Smadja-Lamère, N., Boulanger, M.-C., Champagne, C., Branton, P. E. & Lavoie, J. N. JNK-mediated Phosphorylation of Paxillin in Adhesion Assembly and Tension-induced Cell Death by the Adenovirus Death Factor E4orf4. *J. Biol. Chem.* **283**, 34352–34364 (2008).
22. Branton, P. E. & Roopchand, D. E. The role of adenovirus E4orf4 protein in viral replication and cell killing. *Oncogene* **20**, 7855–7865 (2001).
23. Lu, Y. *et al.* Interaction of Adenovirus Type 5 E4orf4 with the Nuclear Pore Subunit Nup205 Is Required for Proper Viral Gene Expression. *J. Virol.* **88**, 13249–13259 (2014).
24. Groitl, P. & Dobner, T. Construction of adenovirus type 5 early region 1 and 4 virus mutants. *Methods Mol. Med.* **130**, 29–39 (2007).
25. Cabon, L. *et al.* Adenovirus E4orf4 Protein-Induced Death of p53−/− H1299 Human Cancer Cells Follows a G1 Arrest of both Tetraploid and Diploid Cells due to a Failure To Initiate DNA Synthesis. *J. Virol.* **87**, 13168–13178 (2013).
26. Sriskandarajah, N., Blanchette, P., Kucharski, T. J., Teodoro, J. G. & Branton, P. E. Analysis by Live Imaging of Effects of the Adenovirus E4orf4 Protein on Passage through Mitosis of H1299 Tumor Cells. *J. Virol.* **89**, 4685–4689 (2015).
27. Kleinberger, T. Induction of Cancer-Specific Cell Death by the Adenovirus E4orf4 Protein. in *Anticancer Genes* (ed. Grimm, S.) 61–97 (Springer, 2014).
28. Mui, M. Z. *et al.* Identification of the Adenovirus E4orf4 Protein Binding Site on the B55α and Cdc55 Regulatory Subunits of PP2A: Implications for PP2A Function, Tumor Cell Killing and Viral Replication. *PLOS Pathog.* **9**, e1003742 (2013).

29. Mui, M. Z. *et al.* The Human Adenovirus Type 5 E4orf4 Protein Targets Two Phosphatase Regulators of the Hippo Signaling Pathway. *J. Virol.* **89**, 8855–8870 (2015).
30. Marcellus, R. C. *et al.* Induction of p53-Independent Apoptosis by the Adenovirus E4orf4 Protein Requires Binding to the Bα Subunit of Protein Phosphatase 2A. *J. Virol.* **74**, 7869–7877 (2000).
31. Wlodarchak, N. & Xing, Y. PP2A as a master regulator of the cell cycle. *Crit. Rev. Biochem. Mol. Biol.* **51**, 162–184 (2016).
32. Zhang, Z. *et al.* Genetic Analysis of B55α/Cdc55 Protein Phosphatase 2A Subunits: Association with the Adenovirus E4orf4 Protein. *J. Virol.* **85**, 286–295 (2011).
33. Garcia, A. *et al.* Serine/threonine protein phosphatases PP1 and PP2A are key players in apoptosis. *Biochimie* **85**, 721–726 (2003).
34. Jayadeva, G. *et al.* B55α PP2A Holoenzymes Modulate the Phosphorylation Status of the Retinoblastoma-related Protein p107 and Its Activation. *J. Biol. Chem.* **285**, 29863–29873 (2010).
35. Guergnon, J. *et al.* PP2A targeting by viral proteins: A widespread biological strategy from DNA/RNA tumor viruses to HIV-1. *Biochim. Biophys. Acta BBA - Mol. Basis Dis.* **1812**, 1498–1507 (2011).
36. Chroboczek, J., Bieber, F. & Jacrot, B. The sequence of the genome of adenovirus type 5 and its comparison with the genome of adenovirus type 2. *Virology* **186**, 280–285 (1992).
37. Rios, P., Li, X. & Köhn, M. Molecular mechanisms of the PRL phosphatases. *FEBS J.* **280**, 505–524 (2013).

38. Chen, Y. S. *et al.* Mg2+-ATP Sensing in CNNM, a Putative Magnesium Transporter. *J. Biol. Chem.* **293**, 19998–20007 (2018).
39. Arjona, F. J. & de Baaij, J. H. F. CrossTalk opposing view: CNNM proteins are not Na+/Mg2+ exchangers but Mg2+ transport regulators playing a central role in transepithelial Mg2+ (re)absorption. *J. Physiol.* **596**, 747–750 (2018).
40. Schäffers, O. J. M., Hoenderop, J. G. J., Bindels, R. J. M. & de Baaij, J. H. F. The rise and fall of novel renal magnesium transporters. *Am. J. Physiol. Renal Physiol.* **314**, F1027–F1033 (2018).
41. Giménez-Mascarell, P. *et al.* Current Structural Knowledge on the CNNM Family of Magnesium Transport Mediators. *Int. J. Mol. Sci.* **20**, 1135 (2019).
42. Funato, Y. & Miki, H. Molecular function and biological importance of CNNM family Mg2+ transporters. *J. Biochem. (Tokyo)* **165**, 219–225 (2019).
43. Yamazaki, D. *et al.* Basolateral Mg2+ Extrusion via CNNM4 Mediates Transcellular Mg2+ Transport across Epithelia: A Mouse Model. *PLoS Genet.* **9**, e1003983 (2013).
44. Arjona, F. J. *et al.* CNNM2 Mutations Cause Impaired Brain Development and Seizures in Patients with Hypomagnesemia. *PLoS Genet.* **10**, (2014).
45. Accogli, A. *et al.* CNNM2 homozygous mutations cause severe refractory hypomagnesemia, epileptic encephalopathy and brain malformations. *Eur. J. Med. Genet.* **62**, 198–203 (2019).
46. Parry, D. A. *et al.* Mutations in CNNM4 Cause Jalili Syndrome, Consisting of Autosomal-Recessive Cone-Rod Dystrophy and Amelogenesis Imperfecta. *Am. J. Hum. Genet.* **84**, 266–273 (2009).

47. Gómez-García, I. *et al.* Purification, crystallization and preliminary crystallographic analysis of the CBS-domain pair of cyclin M2 (CNNM2). *Acta Crystallograph. Sect. F Struct. Biol. Cryst. Commun.* **68**, 1198–1203 (2012).
48. Baykov, A. A., Tuominen, H. K. & Lahti, R. The CBS domain: a protein module with an emerging prominent role in regulation. *ACS Chem. Biol.* **6**, 1156–1163 (2011).
49. Corral-Rodríguez, M. Á. *et al.* Nucleotide binding triggers a conformational change of the CBS module of the magnesium transporter CNNM2 from a twisted towards a flat structure. *Biochem. J.* **464**, 23–34 (2014).
50. Chen, Y. S. *et al.* The cyclic nucleotide–binding homology domain of the integral membrane protein CNNM mediates dimerization and is required for Mg2+ efflux activity. *J. Biol. Chem.* **293**, 19998–20007 (2018).
51. Hirata, Y., Funato, Y., Takano, Y. & Miki, H. Mg2+-dependent Interactions of ATP with the Cystathionine-β-Synthase (CBS) Domains of a Magnesium Transporter. *J. Biol. Chem.* **289**, 14731–14739 (2014).
52. Bai, Y. *et al.* Novel Anticancer Agents Based on Targeting the Trimer Interface of the PRL Phosphatase. *Cancer Res.* **76**, 4805–4815 (2016).
53. Hardy, S. *et al.* Physiological and oncogenic roles of the PRL phosphatases. *FEBS J.* **285**, 3886–3908 (2018).
54. Rubio, T. & Köhn, M. Regulatory mechanisms of phosphatase of regenerating liver (PRL)-3. *Biochem. Soc. Trans.* **44**, 1305–1312 (2016).
55. Gungabeesoon, J., Tremblay, M. L. & Uetani, N. Localizing PRL-2 expression and determining the effects of dietary Mg2+ on expression levels. *Histochem. Cell Biol.* **146**, 99–111 (2016).

56. Hardy, S. *et al.* The protein tyrosine phosphatase PRL-2 interacts with the magnesium transporter CNNM3 to promote oncogenesis. *Oncogene* **34**, 986–995 (2015).
57. Bessette, D. C., Qiu, D. & Pallen, C. J. PRL PTPs: mediators and markers of cancer progression. *Cancer Metastasis Rev.* **27**, 231–252 (2008).
58. Hardy, S., Wong, N. N., Muller, W. J., Park, M. & Tremblay, M. L. Overexpression of the protein tyrosine phosphatase PRL-2 correlates with breast tumor formation and progression. *Cancer Res.* **70**, 8959–8967 (2010).
59. Kostantin, E. *et al.* Inhibition of the PRL-2/CNNM3 Protein Complex Formation Decreases Breast Cancer Proliferation and Tumor Growth. *J. Biol. Chem.* (2016).
60. Zeng, Q. *et al.* PRL-3 and PRL-1 Promote Cell Migration, Invasion, and Metastasis. *Cancer Res.* **63**, 2716–2722 (2003).
61. Hardy, S. *et al.* Magnesium-sensitive upstream ORF controls PRL phosphatase expression to mediate energy metabolism. *Proc. Natl. Acad. Sci.* **116**, 2925–2934 (2019).
62. Uetani, N. *et al.* PRL2 links magnesium flux and sex-dependent circadian metabolic rhythms. *JCI Insight* **2**, (2017).
63. Yoshida, A., Funato, Y. & Miki, H. Phosphatase of regenerating liver maintains cellular magnesium homeostasis. *Biochem. J.* **475**, 1129–1139 (2018).
64. Matsuda-Lennikov, M. *et al.* Magnesium transporter 1 (MAGT1) deficiency causes selective defects in N-linked glycosylation and expression of immune-response genes. *J. Biol. Chem.* **294**, 13638–13656 (2019).

65. Ikari, A. *et al.* Magnesium deficiency suppresses cell cycle progression mediated by increase in transcriptional activity of p21(Cip1) and p27(Kip1) in renal epithelial NRK-52E cells. *J. Cell. Biochem.* **112**, 3563–3572 (2011).
66. Nielsen, F. H. Dietary Magnesium and Chronic Disease. *Adv Chronic Kidney Dis* **25**, 230–235 (2018).
67. Ismail, A. A. A., Ismail, Y. & Ismail, A. A. Chronic magnesium deficiency and human disease; time for reappraisal? *QJM Int. J. Med.* **111**, 759–763 (2018).
68. Trapani, V. & Wolf, F. I. Dysregulation of Mg2+ homeostasis contributes to acquisition of cancer hallmarks. *Cell Calcium* **83**, 102078 (2019).
69. Hartwig, A. Role of magnesium in genomic stability. *Mutat. Res. Mol. Mech. Mutagen.* **475**, 113–121 (2001).
70. Romani, A. M. P. Cellular Magnesium Homeostasis. *Arch. Biochem. Biophys.* **512**, 1–23 (2011).
71. Zou, Z.-G., Rios, F. J., Montezano, A. C. & Touyz, R. M. TRPM7, Magnesium, and Signaling. *Int. J. Mol. Sci.* **20**, 1877 (2019).
72. Nikonorova, I. A., Kornakov, N. V., Dmitriev, S. E., Vassilenko, K. S. & Ryazanov, A. G. Identification of a Mg2+-sensitive ORF in the 5'-leader of TRPM7 magnesium channel mRNA. *Nucleic Acids Res.* **42**, 12779–12788 (2014).
73. Williams, J. F. Enhancement of Adenovirus Plaque Formation on HeLa Cells by Magnesium Chloride. *J. Gen. Virol.* **9**, 251–255 (1970).

74. Barahona, H. H. & Hanson, R. P. Plaque Enhancement of Newcastle Disease Virus (Lentogenic Strains) by Magnesium and Diethylaminoethyl Dextran. *Avian Dis.* **12**, 151–158 (1968).

75. Wallis, C., Morales, F., Powell, J. & Melnick, J. L. Plaque Enhancement of Enteroviruses by Magnesium Chloride, Cysteine, and Pancreatin. *J. Bacteriol.* **91**, 1932–1935 (1966).

76. Fiala, M. & Kenny, G. E. Effect of Magnesium on Replication of Rhinovirus HGP. *J. Virol.* **1**, 489–493 (1967).

77. Sohn, S.-Y. & Hearing, P. Adenoviral strategies to overcome innate cellular responses to infection. *FEBS Lett.* **593**, 3484–3495 (2019).

78. Lam, E. & Falck-Pedersen, E. Unabated Adenovirus Replication following Activation of the cGAS/STING-Dependent Antiviral Response in Human Cells. *J. Virol.* **88**, 14426–14439 (2014).

79. Zheng, Y., Stamminger, T. & Hearing, P. E2F/Rb Family Proteins Mediate Interferon Induced Repression of Adenovirus Immediate Early Transcription to Promote Persistent Viral Infection. *PLOS Pathog.* **12**, e1005415 (2016).

80. Li, S. *et al.* Type I Interferons: Distinct Biological Activities and Current Applications for Viral Infection. *Cell. Physiol. Biochem.* **51**, 2377–2396 (2018).

81. Wolf, F. I., Di Francesco, A., Covacci, V. & Cittadini, A. Regulation of magnesium efflux from rat spleen lymphocytes. *Arch. Biochem. Biophys.* **344**, 397–403 (1997).

82. Ullman, A. J., Reich, N. C. & Hearing, P. Adenovirus E4 ORF3 protein inhibits the interferon-mediated antiviral response. *J. Virol.* **81**, 4744–4752 (2007).

83. Weitzman, M. D. & Ornelles, D. A. Inactivating intracellular antiviral responses during adenovirus infection. *Oncogene* **24**, 7686–7696 (2005).

84. Look, D. C. *et al.* Direct Suppression of Stat1 Function during Adenoviral Infection. *Immunity* **9**, 871–880 (1998).

85. Olanubi, O., Frost, J. R., Radko, S. & Pelka, P. Suppression of Type I Interferon Signaling by E1A via RuvBL1/Pontin. *J. Virol.* **91**, (2017).

86. Hidalgo, P., Ip, W. H., Dobner, T. & Gonzalez, R. A. The biology of the adenovirus E1B 55K protein. *FEBS Lett.* **593**, 3504–3517 (2019).

87. Horwitz, M. S. Function of adenovirus E3 proteins and their interactions with immunoregulatory cell proteins. *J. Gene Med.* **6**, S172–S183 (2004).

88. Reich, N. C., Sarnow, P., Duprey, E. & Levine, A. J. Monoclonal antibodies which recognize native and denatured forms of the adenovirus DNA-binding protein. *Virology* **128**, 480–484 (1983).

89. Philipson, L. Adenovirus assay by the fluorescent cell-counting procedure. *Virology* **15**, 263–268 (1961).

90. Rueden, C. T. *et al.* ImageJ2: ImageJ for the next generation of scientific image data. *BMC Bioinformatics* **18**, 529 (2017).

91. Schindelin, J. *et al.* Fiji - an Open Source platform for biological image analysis. *Nat. Methods* **9**, (2012).

92. Thomas, P. & Smart, T. G. HEK293 cell line: A vehicle for the expression of recombinant proteins. *J. Pharmacol. Toxicol. Methods* **51**, 187–200 (2005).

93. Kjellén, L. A study of adenovirus-host cell system by the plaque technique. *Virology* **14**, 234–239 (1961).

94. Taylor, S. C. & Posch, A. The Design of a Quantitative Western Blot Experiment. *BioMed Res. Int.* **2014**, (2014).

95. Harlow, E., Franza, B. R. & Schley, C. Monoclonal antibodies specific for adenovirus early region 1A proteins: extensive heterogeneity in early region 1A products. *J. Virol.* **55**, 533–546 (1985).

96. Lavoie, J. N., Nguyen, M., Marcellus, R. C., Branton, P. E. & Shore, G. C. E4orf4, a Novel Adenovirus Death Factor That Induces p53-independent Apoptosis by a Pathway That Is Not Inhibited by zVAD-fmk. *J. Cell Biol.* **140**, 637–645 (1998).

97. Boivin, D., Morrison, M. R., Marcellus, R. C., Querido, E. & Branton, P. E. Analysis of Synthesis, Stability, Phosphorylation, and Interacting Polypeptides of the 34-Kilodalton Product of Open Reading Frame 6 of the Early Region 4 Protein of Human Adenovirus Type 5. *J. Virol.* **73**, 1245–1253 (1999).

98. Mittermeier, L. *et al.* TRPM7 is the central gatekeeper of intestinal mineral absorption essential for postnatal survival. *Proc. Natl. Acad. Sci. U. S. A.* **116**, 4706–4715 (2019).

99. Leclerc, G. M., Boockfor, F. R., Faught, W. J. & Frawley, L. S. Development of a Destabilized Firefly Luciferase Enzyme for Measurement of Gene Expression. *BioTechniques* **29**, 590–601 (2000).

100. Ross, P. J. *et al.* Assembly of Helper-Dependent Adenovirus DNA into Chromatin Promotes Efficient Gene Expression. *J. Virol.* **85**, 3950–3958 (2011).

101. Badralmaa, Y. & Natarajan, V. Impact of the DNA extraction method on 2-LTR DNA circle recovery from HIV-1 infected cells. *J. Virol. Methods* **193**, 184–189 (2013).

102. Livak, K. J. & Schmittgen, T. D. Analysis of relative gene expression data using real-time quantitative PCR and the 2(-Delta Delta C(T)) Method. *Methods San Diego Calif* **25**, 402–408 (2001).

103. Meier, O. & Greber, U. F. Adenovirus endocytosis. *J. Gene Med.* **6**, S152–S163 (2004).

104. Murphy, E. & London, R. E. A practical guide to the use of fluorescent indicators for the measurement of sytosolic free magnesium. *Methods Neurosci.* 304–318 (1995).

105. Watanabe, M. & Konishi, M. Intracellular calibration of the fluorescent Mg2+ indicator furaptra in rat ventricular myocytes. *Pflüg. Arch.* **442**, 35–40 (2001).

106. Shi, W.-Y., Cao, C. & Liu, L. Interferon α Induces the Apoptosis of Cervical Cancer HeLa Cells by Activating both the Intrinsic Mitochondrial Pathway and Endoplasmic Reticulum Stress-Induced Pathway. *Int. J. Mol. Sci.* **17**, 1832 (2016).

107. Lau, L., Gray, E. E., Brunette, R. L. & Stetson, D. B. DNA tumor virus oncogenes antagonize the cGAS-STING DNA-sensing pathway. *Science* **350**, 568–571 (2015).

108. Miron, M.-J., Gallouzi, I.-E., Lavoie, J. N. & Branton, P. E. Nuclear localization of the adenovirus E4orf4 protein is mediated through an arginine-rich motif and correlates with cell death. *Oncogene* **23**, 7458–7468 (2004).

109. Li, J. *et al.* Virus-Host Interactome and Proteomic Survey Reveal Potential Virulence Factors Influencing SARS-CoV-2 Pathogenesis. *Med* **2**, 99-112.e7 (2021).